Phosphogypsum as additive for foamed bitumen manufacturing used in asphalt paving

A.A. Cuadri [a,*], S. Pérez-Moreno [b], C.L. Altamar [b], F.J. Navarro [a], J.P. Bolívar [b]

[a] *Department of Chemical Engineering, Chemical Product and Process Technology Research Center-Pro^{2}TecS, University of Huelva, 21071, Huelva (Spain).*

[b] *Department of Integrated Sciences, Center for Natural Resources, Health and Environment (RENSMA), University of Huelva, 21071, Huelva (Spain).*

[*] Author to whom correspondence should be addressed:

Dr. Antonio Abad Cuadri

E-mail: antonio.cuadri@diq.uhu.es

Phone: +34 959 21 9882

Fax: +34 959 21 99 83

ABSTRACT

The aim of this work was to use phosphogypsum (FY) waste in a sustainable paving practice involving the production of FY-foamed bitumen for road applications. For this proposal, three FY types coming from different fertilizer industries and a reference natural gypsum were used as foaming agents (10 wt.%), including a small quantity of sulfuric acid (0.5 wt.%) in the foamed bitumen formulation. The foaming properties and the rheological characterization of their corresponding binder residues were conducted by a distance laser sensor and by dynamic shear rheology, respectively. In addition, a physicochemical characterization of the used materials was carried out in order to evaluate their role in the final product. Knowing that FY is a Naturally Occurring Radioactive Material (NORM) waste, a comprehensive radioactive characterization, by both alpha and gamma spectrometry, and an environmental evaluation, by a Dynamic Surface Leaching Test (DSLT), were performed to comply with the EU radiological regulation of NORM materials for building materials. In conclusion, FY-foamed bitumen displayed enhanced engineering properties compared to that prepared with the reference natural gypsum, satisfying the radioactive and environmental specifications established according to the EU regulations.

Keywords: Phosphogypsum, foamed bitumen, NORM, environment, building materials

1. INTRODUCTION

Phosphogypsum (FY) is a byproduct generated in the production of phosphoric acid by the wet process (the most common route for its production using sulfuric acid), and contains significant concentrations of impurities (heavy metals, Fluorine, P_2O_5, low pH, etc.) and natural radionuclides from ^{238}U-series (Bolívar et al., 2009; Haque et al., 2020; Huang et al., 2020; Pérez-López et al., 2010; Pérez-Moreno et al., 2018). About 85 % of FY worldwide production (more than 300 Mt every year) ends up stored in regular open stacks, sometimes even near built-up or ecologically sensitive areas, with enormous risks for both human health and the environment (Bolivar et al., 2009; Cuadri et al., 2014; Monat et al., 2020). Although some attempts have been conducted for using FY in the fields of construction (Kacimi et al., 2006; Rosales et al., 2020) or agriculture (Al-Enazy et al., 2018; Karim et al., 2019; Zrelli et al., 2018), the presence of these impurities and U-series radionuclides considerably worsens the final properties of the resulting materials. Therefore, the scientific community is being pressured to propose sustainable process routes for FY valorization.

Focusing on the use of FY waste for construction applications, more precisely, in the asphalt paving industry, the fact that bitumen is considered an environmentally friendly way to immobilize Naturally Occurring Radioactive Material (NORM) radioactive waste like FY (Ojovan and Lee, 2005), opens up novel lines of research for pavement engineers. In this sense, the traditional use of FY waste has been to replace a portion of the mineral aggregate used in the formulation of asphalt mixtures for roads applications (which are composed by a ca. 5/95 wt.% ratio of bitumen/aggregates). In a previous work (Cuadri et al., 2014), it was demonstrated that FY can also act as bitumen modifier when a small quantity of sulfuric acid (0.5 wt.%) is added in the bitumen processing protocol. Thus, FTIR results revealed that sulfuric acid addition at 150 ºC is able to release the phosphorus

61 contained in the crystalline structure of FY, allowing reactions with bitumen's
62 compounds and giving rise to an improvement in the rheological response of the resulting
63 binder.
64 Interestingly, in the present paper, it is proposed the use of FY waste as foaming agents
65 to prepare foamed bitumen for asphalt paving applications. This is possible through the
66 significant waster associated to the molecular structure presents in the FY waste. Foamed
67 bitumen can be obtained either by employing of water bearing additives or by direct
68 addition of water, which is converted to steam, into hot bitumen (Abreu et al., 2017). As
69 an alternative to the production of Hot Mix Asphalt (HMA), which requires mixing the
70 bitumen with aggregates at temperatures up to 180 ºC to obtain an appropriate coating of
71 the mineral, the use of foamed bitumen is considered a sustainable paving practice.
72 It enables a coating at reduced temperatures due to the much higher surface area of foam
73 compared to hot bitumen. Consequently, the use of foamed bitumen in the paving
74 industry, which is framed within the Warm Mix Asphalt techniques, brings with it a
75 reduction of greenhouse gas emissions (Dinis-Almeida and Afonso, 2015), energy
76 savings and an improvement in the safety conditions for operators (Zaumanis et al., 2012).
77 Therefore, this paper proposes the use of FY waste in a sustainable paving practice
78 involving the production of FY-foamed bitumen for road applications. The foaming
79 properties and the rheological characterization of their corresponding binder residues
80 (i.e., the resulting material after the foaming process) were conducted to this end.
81 Furthermore, a physicochemical characterization of used materials was carried out in
82 order to evaluate their key role in the final applicability of this waste for paving
83 applications. In addition to that, a comprehensive radioactivity and environmental
84 implication evaluation were performed to comply with the radioactive specifications

when NORM materials are used in building materials, and with the environmental requirements related to the release of the contaminant substances.

2. EXPERIMENTAL SECTION

2.1. Materials

A bitumen with values of penetration and R&B softening temperature of 55 dmm and 52.4 ºC (according to EN 1426 and EN 1427, respectively) was used as base material for the preparation of foamed binders.

Three phosphogypsum samples and a reference sample of natural gypsum were used as foaming agents for the preparation of the phosphogypsum-foamed binders. On the one hand, the phosphogypsum samples used in this work come from different phosphoric acid production industry installed in various parts in the world, concretely in Spain (referred to as SFY, hereinafter), Tunisia (TFY) and Saudi Arabia (AFY). All samples were taken in different point of their local disposal, with the aim of achieving representative materials. In addition, prior to the analysis, the samples were dried in an oven at 50 °C, in order to avoid the loss of the structural water, and finally they were homogenised. This waster is associated to the molecular structure of compounds, which is lost at temperature higher than 100 ºC. On the other hand, a natural gypsum (NG) sample, supplied by "Grupo Cemento Portlant Valderrivas", was also used to prepare a reference foamed binder. Finally, sulfuric acid, H_2SO_4 (96 wt.%), supplied by Panreac, S.A., was also used in the formulation of the phosphogypsum-foamed binders.

2.2. Foamed binder processing

The general procedure to prepare the foamed binders consisted in mixing molten base bitumen and 10 wt.% of foaming agent (i.e., each FY or NG), in a cylindrical vessel partially submerged in an oil bath, for 15 min at a selected foaming temperature. After this mixing time, 0.5 wt.% sulfuric acid, H_2SO_4, (referred to the total weight of bitumen

and foaming agent) was added to the blend and the agitation was then stopped. At that time, the foaming process starts and the evolution of the foam height with time (up to 600 s) was monitored by a laser device DLS-C 15 distance laser sensor (Dimetix AG) placed on the top of the mixing vessel (Figure 1).

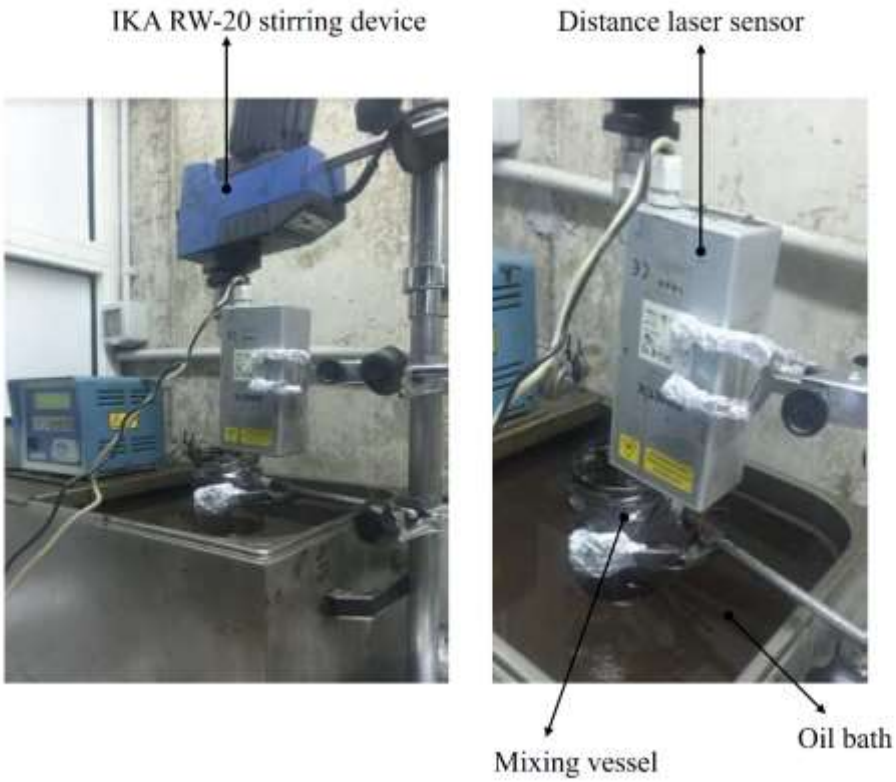

Figure 1. Equipment used to conduct the foaming test and the height foam recording.

In a previous paper (Cuadri et al., 2014) it was demonstrated that the addition of sulfuric acid to bitumen is necessary to the release of phosphorus from the crystalline structure of phosphogypsum. Similarly, foaming process only occurs after sulfuric acid addition to bitumen. Therefore, sulfuric acid could be considered as the "promoting" agent for the release of both phosphorus and structural water containing in the phosphogypsum.

The evolution of the height foam with foaming time (600 s) is used to calculate the expansion ratio (ER) which provides valuable information about the foamability and workability of the resulting mixture (Abreu et al., 2017; Hailesilassie et al., 2015). This

parameter is defined as the ratio of foam volume achieved at each time to the original volume of its bituminous binders before foaming. Since the cross section of the mixing vessel is constant, ER is calculated using the height foam as follows:

$$ER = \frac{V_{foam}}{V_{binder}} = \frac{h_{foam} \cdot S_{vessel}}{h_{binder} \cdot S_{vessel}} = \frac{h_0 - h_t}{h_b} \quad (1)$$

where "h_b" is the initial height of the binder just before foaming starts (i.e., just before sulfuric acid addition), "h_0" is the distance between the laser device and the surface of the binder just before foaming, and "h_t" is the distance the laser sensor device and the surface of the binder for each time during the foaming process. The meaning of these parameters ("h_b", "h_0", "h_t") is illustrated Figure 2.

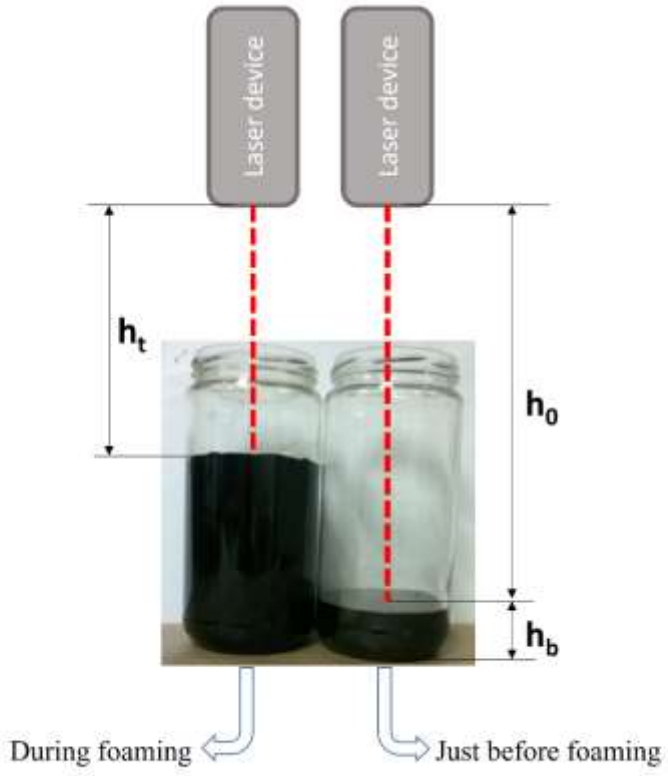

Figure 2. Image illustrating the meaning of the parameters ("h_b", "h_0" and "h_t") used to calculate ER.

136 Once the foaming tests were finished, the foamed binder residue was stored in a freezer
137 for further characterization. In addition, a portion of bituminous blend before sulfuric acid
138 addition (i.e., before foaming) was also taken for its characterization.
139 With the goal to study the influence of phosphogypsum source and foaming temperature
140 on both foaming and binder residues properties, Table 1 gathers the different foaming
141 tests conducted in this work. In addition, to quantity the effects of acid bitumen
142 modification on the properties of the resulting binder residues, three more blends
143 containing only base bitumen and 0.5 wt.% H_2SO_4 were prepared with the same stirring
144 device, for 1 h, at 130, 140 or 150 ºC. These bituminous binders will be referred to as
145 B130, B140 and B150, respectively.

146 **Table 1.** Nomenclature, foaming agent and foaming temperature used for the
147 preparation of the foamed binders.

Nomenclature	Phosphogypsum	Foaming temperature (ºC)
NG150	Natural gypsum (NG)	150
SA150	Saudi Arabia (AFY)	150
T150	Tunisia (TFY)	150
S150	Spain (SFY)	150
S140	Spain (SFY)	140
S130	Spain (SFY)	130

148

149 Finally, a rubbery polymer/bitumen blend (SBS, hereinafter) prepared with 3 wt.% of
150 styrene-butadiene-styrene Kraton D1101 was also processed by using a Silverson L5M
151 homogenizer at 180 ºC, for 2 h and 6000 rpm. This polymer concentration is typically
152 used for paving applications.

153 **2.3. Pretreatment and physicochemical characterization**

154 In order to achieve accurate rheological measurements, the gap size of a rheometer device
155 must be at least ten times the maximal particle size (de Sousa Mendes at al., 2014).
156 Therefore, FY and NG samples were subjected to a reduction of grain size by grinding in
157 a mortar, with the aim of avoiding the presence of particles larger than 100 µm. In this

158 sense, the samples under study were mostly classified as silt (50-60 %, 4-62 µm) and sand
159 (30-40 %, 62-100 µm), with a maximum in the particle distribution (% volume) about 70
160 µm. The particle size range was determined by laser diffraction analysis through
161 Matersizer 2000 equipment. A representative amount of each sample was placed in water
162 and subjected to ultrasound for 10 min, followed by magnetic stirring for approximately
163 30 min.

164 In addition, the samples were subjected to a chemical characterization using different
165 analytical techniques. The major elements were determined by X-Ray Fluorescence with
166 a Panalytical Axios XRF equipment. The measurement method used was
167 semiquantitative for flat solid samples with a diameter greater than 25 mm. Mass
168 Spectrometry (Perkin Elmer Sciex ELAN 9000 equipment) and Optical Emission (Varian
169 735 ES instrument) Spectrometry with Inductively Coupled Plasma (ICP-MS / OES)
170 were used to trace element quantification. Prior to analysis, samples were digested by
171 combining four acids (hydrochloric, nitric, perchloric and hydrofluoric). The crystalline
172 phases were determined by X-ray diffraction using Panalytical XractPert Pro
173 diffractometer. The minerals identification was performed using an X'PertHighScore
174 Plus Software with PDF-4 ICDD database, and the quantification using the Rietveld
175 method. The amount of structural water was analysed by thermobalance Q-50 from TA
176 Instruments. The operating conditions used were 25-600 ºC with a heating rate of 10 ºC
177 min^{-1} and an inert atmosphere of N_2 with a flow of 50 $mL \cdot min^{-1}$.
178 All techniques and methodologies have been previously validated using blank samples,
179 reference materials and replicates to guarantee the measured absolute values and the
180 reproducibility of the measurements.

181 **2.4. Radioactive characterization**

The activity concentrations of natural radionuclides were measured by alpha spectrometry ($^{234\text{-}238}$U, $^{230\text{-}232}$Th, and ^{210}Po) using ion implantation Si (PIPS) semiconductor detectors, EG & G Ortec. The isolation of radionuclides was performed by a sequential radiochemical procedure with tributylphosphate (TBP) and ion chromatographic resins. Then, the alpha source was prepared by electrodeposition ($^{234\text{-}238}$U, $^{230\text{-}232}$Th) in stainless-steel discs and self-deposited onto silver disks (^{210}Po). Furthermore, gamma spectrometry was also employed (^{210}Pb, $^{226\text{-}228}$Ra and ^{40}K) using an Extended Range (XtRa) coaxial Ge Camberra detector GX3519.

2.5. Environmental characterization

The release of the contaminant substances from the binder residues here obtained was evaluated according to CEN/TS 16637-2:2014 (Construction products - Assessment of release of dangerous substances) specification of the European Commission for construction products. This regulation specifies a Dynamic Surface Leaching Test (DSLT) which is aimed at determining the release per unit surface area as a function of time of inorganic substances from a monolithic when it is put into contact with an aqueous solution (leachant). The leaching test was performed in duplicate for each binder residue, in order to assess the repeatability of the procedure.

DSLT methods applies to regular shaped test portions consisting of monolithic test pieces with minimum dimension of 40 mm in all directions (volume $\geq$ 64 cm^3). The test portion of the product is placed in a 1L leaching vessel of High Density Polyethylene (HDPE) and the exposed surface is completely submerged in demineralized water, which is used as leachant solution. The space between the exposed surfaces of the test portion and the inner walls of the leaching vessel was at least 20 mm as recommended. The leachant is introduced in the leaching vessel up to given volume of liquid to surface are ratio (L/A) of 80 ± 10 L m^{-2}, renewing the leachant at predetermined time intervals (Table 2). Then,

the eluate in each step is removed from the leaching vessel, being pH and electrical conductivity measured immediately. These parameters were determined using a probe portable multiparametric CRISON MM40+. The eluate is filtered and reserved for analysis. In addition, a blank test is carried out follow the same procedure, in order to detect, as far as possible, contamination from equipment and reagents.

Table 2. Renewal times of the leachant according to CEN/TS 16637-2:2014.

Step/fraction	Duration of the specific step	Duration from the start of the test
1	6 h ± 15 min	6 h
2	18 h ± 15 min	1 day (d)
3	1 d and 6 h ± 45 min	2 d and 6 h
4	1 d and 18 h ± 75 min	4 d
5	5 d ± 75 min	9 d
6	7 d ± 75 min	16 d

The eluates were analyzed by ICP-MS and alpha spectrometry. The analysis provides the value of the concentration of the substances in the eluates of the individual time steps. The accumulative released concentration for each element "C_t" is defined as the sum of the concentration in each step (from step 1 to step 6) and can be expressed by the next expression:

$$C_t = \sum_{i=1}^{n} C_i \quad (2)$$

Where "period i" defined the leaching step "i"; "n" is the total steps; "C_i" is the concentration of a substance in eluate, in µg/L. In addition, the accumulative area released (R_n), total quantity of a substance released per area, were calculated for each substance (in mg m^{-2} geometric surface area of the specimen), using the volume (V) of the leachant agent in L, and the area (A) of the test portion, in m^2.

$$R_n = C_t \cdot \frac{V}{A} \quad (3)$$

Finally, the transfer factor (η_j) for a substance ''j'' is defined as the released mass of each substance in relation to its initial mass in the material, and it is given by the following equation:

$$\eta_j(\%) = \frac{C_t \cdot V}{C_0 \cdot m} \cdot 100 \quad (4)$$

Where "C_t" is the accumulative released concentration of a substance (in µg/L), "V" is the leachate volume (in L), "C_0" is the concentration of a substance in the tested specimen (in µg/kg), and "m" their mass employed in each blend (in kg).

2.6. Rheological characterization

In order to evaluate the applicability of this foamed asphalt technology for paving applications, it is essential to measure the rheological properties of the binder residues (i.e., residue after foaming), since it will be the final binder forming the paving material. To that end, a controlled-stress rheometer Physica MCR-301 (1 mm gap and 25 mm plate-plate geometry) was used. Two rheological tests were performed: a) viscous flow curves, at 60 and 135 ºC; and b) temperature sweep tests in oscillatory shear mode, at 10 rad s^{-1} and within the linear viscoelastic interval (1 % strain), from 30 to 100 ºC, at a heating ramp of 1 ºC min^{-1}. For the sake of comparison, bitumen samples just before sulfuric acid addition (i.e., before foaming), rubbery binder (SBS) and samples containing bitumen and sulfuric acid (B130, B140 and B150) were also measured. In order to assure the repeatability of the rheological results, at least three replicates were performed on every bituminous binder studied.

3. RESULTS AND DISCUSSION

3.1. Physicochemical characterization

The physicochemical characterization of the different FY types and the NG includes the mineral composition (Table 3), major and trace elements (Table 4), and the thermogravimetric analysis (Table 5).

251 **Table 3.** Mineral composition (%) for the different phosphogypsum types and the
252 natural gypsum.

Mineral Specie	SFY	TFY	AFY	NG
Gypsum ($CaSO_4 \cdot 2H_2O$)	95.0	75.7	9.6	88.5
Anhydrite ($CaSO_4$)	3.6	ND	7.3	ND
Bassanite ($CaSO_4 \cdot 1/2H_2O$)	ND	ND	79.3	ND
Quartz (SiO_2)	1.3	17.8	3.7	0.9
Dolomite ($CaMg(CO_3)_2$)	ND	ND	ND	10
Illite ($(K,H_3O)(Al, Mg, Fe)_2(Si, Al)_4O_{10}$)	ND	ND	ND	0.6
Apatite ($Ca_5 (PO_4)_3$ (F, Cl, OH))	ND	6.5	ND	ND

253 ND: Not Detected
254

255 **Table 4.** Major and trace elements composition of the different phosphogypsum types
256 and the natural gypsum.

Element	Unit	Detection Limit (DL)	SFY	TFY	AFY	NG	(*)
Al	%	0.01	0.08 ± 0.08	0.51 ± 0.10	0.12 ± 0.04	1.43 ± 0.07	4.1
Ca	%	0.01	22.5 ± 1.1	22.5 ± 1.1	25.2 ± 1.1	15.7 ± 0.8	2.6
F	%	0.01	1.26 ± 0.06	NM	1.37 ± 0.48	< DL	0.06
Fe	%	0.01	0.03 ± 0.03	0.29 ± 0.06	0.09 ± 0.02	0.95 ± 0.19	3.7
Mg	%	0.01	< DL	0.07 ± 0.02	0.03 ± 0.01	2.23 ± 0.11	1.5
Na	%	0.01	0.07 ± 0.07	0.39 ± 0.08	0.12 ± 0.07	0.03 ± 0.03	2.4
P	%	0.01	0.22 ± 0.04	3.51 ± 0.18	0.74 ± 0.21	0.01 ± 0.01	0.07
K	%	0.01	< DL	0.13 ± 0.03	0.05 ± 0.02	0.90 ± 0.18	2.3
S	%	0.01	16.7 ± 0.84	18.5 ± 0.9	17.6 ± 0.7	9.73 ± 0.49	0.06
Si	%	0.01	0.40 ± 0.08	11.3 ± 0.6	1.74 ± 0.28	3.34 ± 0.17	31
Ti	%	0.01	0.02 ± 0.05	0.02 ± 0.02	0.03 ± 0.03	0.10 ± 0.02	0.38
LOI	%	-	23.7	12.3	13.4	37.3	-
Ag	ppm	0.05	0.5 ± 0.1	0.53 ± 0.11	0.27 ± 0.05	< DL	0.05
As	ppm	0.1	6.4 ± 1.3	8.70 ± 1.7	1.90 ± 0.90	1.40 ± 0.30	5.7
B	ppm	1	NM	10.0 ± 2.0	NM	NM	47
Ba	ppm	1	47.0 ± 9.4	43.0 ± 8.6	45.0 ± 9.0	118 ± 6	628
Cd	ppm	0.1	1.30 ± 0.26	80.2 ± 4.0	0.65 ± 0.21	< DL	0.09
Co	ppm	0.1	< DL	0.60 ± 0.60	0.21 ± 0.21	3.50 ± 0.70	15
Cr	ppm	0.5	15.9 ± 0.8	112 ± 5.6	10.0 ± 3.0	29.5 ± 1.5	73
Cu	ppm	0.2	5.2 ± 1.0	9.00 ± 1.80	2.00 ± 1.00	6.30 ± 1.30	27
Hg	ppm	0.01	0.06 ± 0.06	0.33 ± 0.07	NM	0.04 ± 0.04	0.05
Mn	ppm	1	17.0 ± 3.4	35.0 ± 7.0	24.0 ± 8.0	199 ± 10	603
Mo	ppm	0.05	0.68 ± 0.14	4.10 ± 0.20	NM	0.78 ± 0.16	0.6
Ni	ppm	0.5	2.2 ± 0.4	8.20 ± 1.64	1.30 ± 0.40	10.3 ± 0.5	34
Pb	ppm	0.5	5.3 ± 1.1	11.8 ± 0.6	1.7 ± 0.2	5.70 ± 1.10	17
Sb	ppm	0.1	0.10 ± 0.10	< DL	NM	0.50 ± 0.50	0.75
Se	ppm	0.1	< DL	11.2 ± 0.6	NM	0.20 ± 0.20	0.09
Sn	ppm	1	< DL	< DL	NM	< DL	2.2
Sr	ppm	0.2	376 ± 19	916 ± 46	226 ± 13	> 1000	320

Th	ppm	0. 1	0.60 ± 0.12	2.80 ± 0.6	0.19 ± 0.07	2.30 ± 0.46	11
U	ppm	0.1	4.60 ± 0.92	12.4 ± 0.6	8.8 ± 1.9	7.50 ± 1.5	2.7
V	ppm	1	3.0 ± 3.0	14.0 ± 2.8	NM	27.0 ± 5.4	106
Zn	ppm	0.2	10.5 ± 0.5	652 ± 33	15.2 ± 1.0	18.1 ± 0.91	75

NM: Not Measured

(*) Average composition of the upper continental crust (Hu and Gao, 2008).

Table 5. Thermogravimetric analysis data of the different phosphogypsum types and the natural gypsum.

Sample	Peak (ºC)	Temperature range (°C)	Lost mass (%)	Lost Specie
SFY	131	78-155	18.5	H_2O
TFY	129	97-150	11.4	H_2O
AFY	84	50-100	3.1	H_2O
	120	100-140	5.3	H_2O
NG	122	84-152	13.4	H_2O
	512	480-530	1.2	CO_2

The phosphogypsum generated in the Spanish facility (SFY) contains gypsum (95 % $CaSO_4 \cdot 2H_2O$) as principal mineral fraction, containing 18.5 % of structural water. This fact is mainly related to their major elements content, 22.5 ± 1.1 % of Ca and 16.7 ± 0.84 % of S. As, Cd, Cr, Cu, Ni, Pb, Sr and Zn are some of the trace elements found on its composition.

In the phosphogypsum from Tunisia industry (TFY), the main mineral fraction is also gypsum (75.7 % $CaSO_4 \cdot 2H_2O$), but quartz (17.8 % SiO_2) and apatite ($(Ca_5(PO_4)_3(F,Cl,OH))$) are also presented. A not complete of digestion during the process justify the presence of apatite, while quartz is refractory material and is not digested by sulfuric acid. The proportion of these species confirm the major elements composition: Ca (22.5 ± 1.1 %), S (18.5 ± 0.9 %), Si (11.3 ± 0.6 %) and P (3.51 ± 0.18 %, associated with apatite mineral). It has been determined that the structural water in the sample is 11.4 %. In respect of the trace element, As, Cd, Cr, Cu, Ni, Pb, Se, Sr and Zn are detected.

277 The mineral phases presented in the phosphogypsum from Saudi Arabia (AFY) are 79.3
278 % of bassanite ($CaSO_4 \cdot 1/2H_2O$), 9.6 % of gypsum ($CaSO_4 \cdot 2H_2O$), 7.3 % of anhydrite
279 ($CaSO_4$) and 3.7 % quartz (SiO_2). The presence of these species is related to the
280 proportion of the major elements found, 25.2 ± 1.1 % of Ca, 17.6 ± 0.7 % of S and 1.74
281 ± 0.28 % of Si. In addition, As, Cd, Cr, Cu, Ni, Pb, Sr and Zn were detected. The total
282 quantity of the structural water is 8.4 %.
283 The NG is composed of 88.5 % of gypsum ($CaSO_4 \cdot 2H_2O$) and 10 % of dolomite
284 ($CaMg(CO_3)_2$) as main mineral phases. The major element concentration is related to
285 these mineral phases, while As, Cr, Cu, Ni, Pb and Zn are detected as trace element. The
286 structural water is 13.4 % of the total sample.

287 **3.2. Foamability and rheological characterization of foamed binder residues**

288 **3.2.1. Effects of foaming temperature on foamability**

289 With the objective to evaluate the effects of foaming temperature on foamability, foaming
290 tests at three different temperature (130, 140 and 150 ºC) were conducted on the binders
291 prepared with the phosphogypsum of Spain (SFY). This FY was selected for this study
292 since it displayed the highest structural water content of all. The ER is the typical
293 parameter for evaluating the foamability, since it is related to the viscosity of the foam
294 and, thereby, to the wettability of the foamed bitumen and the workability of the resulting
295 mixture (Abreu et al., 2017; Hailesilassie et al., 2015). Figure 3 shows the evolution of
296 ER with time for these phosphogypsum-foamed binders.

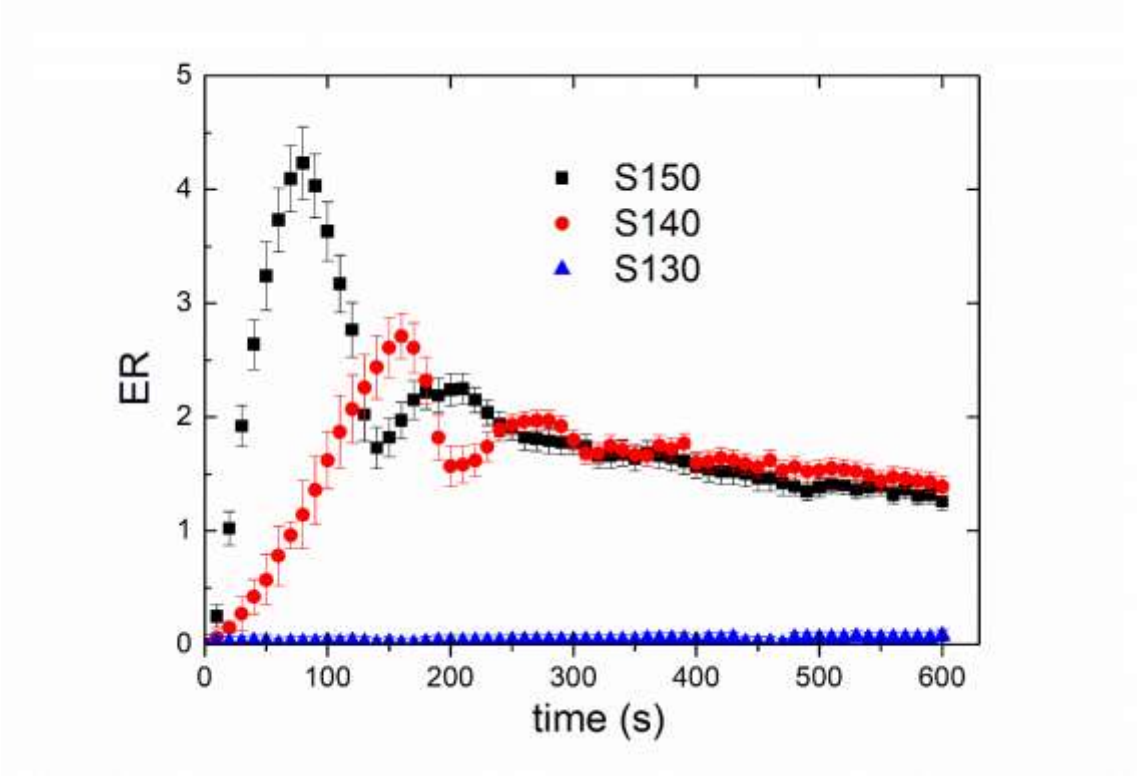

297

298 **Figure 3.** Evolution of expansion ratio (ER) with time for the foamed binders prepared
299 with the phosphogypsum of Huelva (SFY) at three different foaming temperatures (130,
300 140 and 150 ºC).

301 As can be seen, significant differences are observed by changing the foaming
302 temperature. On the one hand, the binders foamed at 140 and 150 ºC (S140 or S150 in
303 Figure 3) present a similar qualitative evolution of ER with time, which is characterized
304 by the appearance of two ER maximums (ER_{max}) and a progressive decay of ER until
305 values higher than 1. However, these maximums appear with less intensity and at higher
306 times for the foam prepared at 140 ºC. On the other hand, at 130 ºC, no foam is created,
307 since ER values remains close to 0 (S130 in Figure 3). In general terms, the foaming
308 properties can be explained on the basis of two combined effects: a) the structural water
309 content of each phosphogypsum, and b) the binder's viscosity just before the foaming
310 starts. With regards to the latter, knowing that bubbles collapse when the elongation limit
311 of the covering film is overlapped, it is expected that a binder with higher viscosity leads

312 to a greater progressive accumulation of unbroken bubbles, resulting in higher values of
313 ER_{max} and t_{max} (He and Wong, 2006). This characteristic time (t_{max}) is the foaming time
314 for which an ER maximum is attained. However, and contrary to what is to be expected,
315 ER_{max} values are considerably reduced when the foaming temperature decreases from 150
316 up to 140 ºC, and no foam is produced at 130 ºC. In this sense, Cuadri et al. (2014)
317 reported that the release of phosphorus from the crystalline structure of phosphogypsum
318 takes place when the addition of sulfuric acid to bitumen occurs at 150 ºC and not at 90
319 ºC. Similarly, we may assume that the release of structural water could be also favoured
320 when the foaming test is carried out at higher temperatures, as deduced from the ER_{max}
321 values for the foam prepared at 150 ºC and 140 ºC (S150 and S140 in Figure 3). In
322 addition, the release of structural water would not be detectable at 130 ºC and,
323 consequently, there is no foaming.

324 **3.2.2. Effects of phosphogypsum source on foamability**

325 With the purpose of exploring the effects of phosphogypsum source on foaming
326 properties, Figure 4 displays the evolution of ER with time for the phosphogypsum-
327 foamed binders prepared at a foaming temperature of 150 ºC using the different FY types
328 (Figures 4A, 4B and 4C).

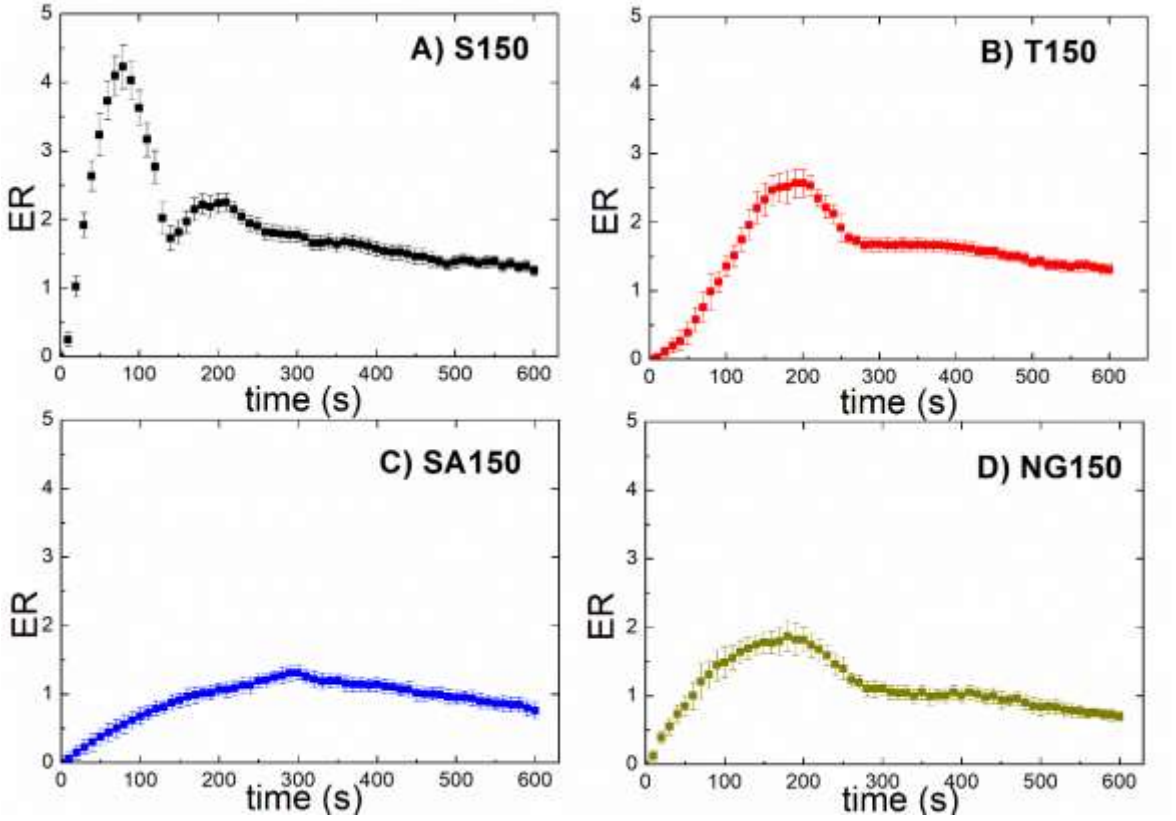

Figure 4. Evolution of expansion ratio (ER) with foaming time for the foamed binders prepared at a foaming temperature of 150 ºC.

This foaming temperature (150 ºC) was selected for this purpose since it resulted in the highest ER_{max} values (see Figure 3). The corresponding curve obtained from the natural gypsum is included as reference (Figure 4D). Although the evolution of ER follows the same general pattern, which is characterized by an increase up to a maximum value (defined by ER_{max} and t_{max}) and then a decay until the final foaming time (600 s), significant differences on their foaming properties can be noticed. Thus, the values of ER_{max}, t_{max} and the foaming rate (i.e., the slope of the curve during the expansion step until ER_{max} is achieved) depend on the FY used to prepare the bituminous binder. Interestingly, the viscosity values at 60 ºC of the three phosphogypsum-binders before foaming are similar (ca. 275 Pa·s), as will also be commented in Figure 6. Therefore, the differences in foaming properties among them should be related to the structural water content of each FY. In order to corroborate this assumption, Figure 5 shows the

dependence of ER_{max} and t_{max} with the structural water content for the three phosphogypsum-foamed binders (those values corresponding to the foam prepared with the natural gypsum has been also included).

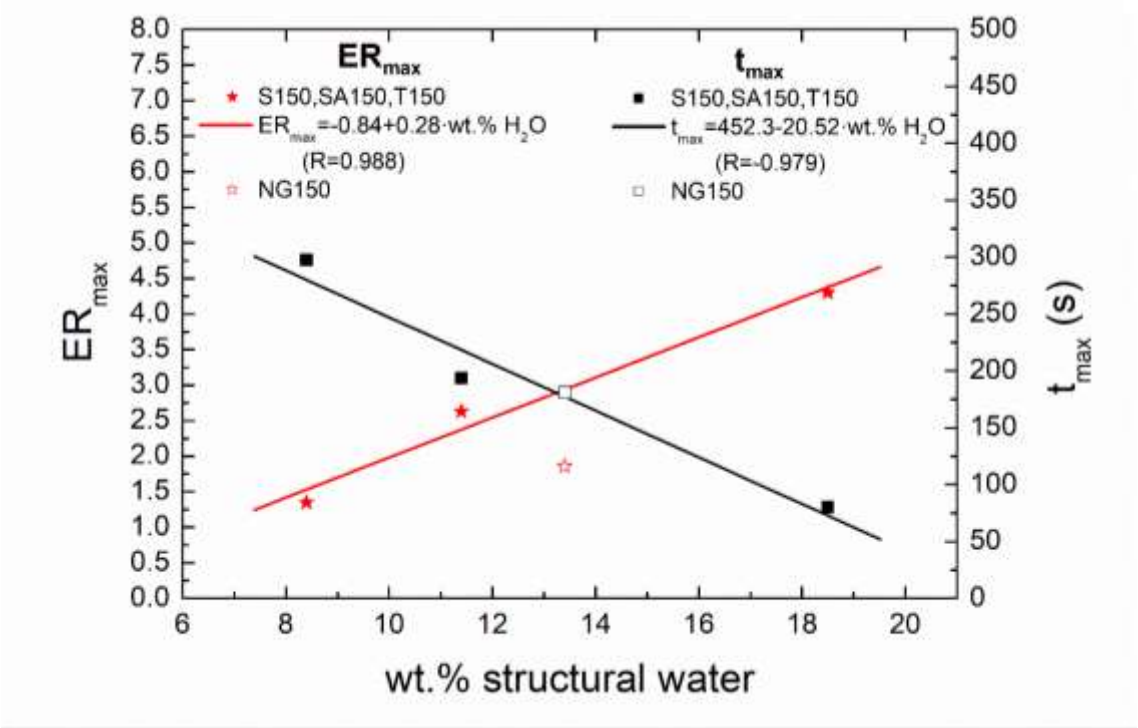

Figure 5. Dependence of ER_{max} and t_{max} with the structural water content for the three phosphogypsum-foamed binders.

From Figure 5, two conclusions of paramount importance can be highlighted: a) on the one hand, the foam takes less time to reach ER_{max} as structural water content increases, as deduced from the lower t_{max} values; b) ER_{max} values increase as structural water content does. In addition, ER_{max} and t_{max} values calculated for the phosphogypsum-foamed binders follow a reasonable good linear fitting with the structural water content.

With regards to the workability of these foamed binders, the time elapsing between the foam reaches ER_{max} and ER≈0 is a measure of the foamed bitumen's stability, and provides valuable information about the time available for its mixture production (Abreu et al., 2017; Hailesilassie et al., 2015). Interestingly, whereas this time for a standard bitumen foaming by water addition is less than 100 s (Abreu et al., 2017; Hailesilassie et

al., 2015), ER value after 600 s of foaming time (Figure 4) is higher than 1 for S150 and T150 samples, and with a value closer to 1 for SA150 and NG150 samples. Thus, when necessary, operators have more time to conduct the lay-down and compaction operations compared to traditional water-foamed bitumen.

3.2.3. Rheological characterization of foamed binder residues

The applicability of this foaming procedure for paving industry was assessed by rheological measurements conducted on the binder residues, since these materials will be the final binders forming the paving material. To that end, viscous flow curves, at 60 and 135 ºC, and temperature sweep tests in oscillatory shear mode were conducted on them.

Figure 6 displays the viscous flow curves, at 60 ºC, for the base bitumen and their corresponding phosphogypsum modified binders prepared at 150 ºC before and after foaming process. This testing temperature is usually considered as the maximum temperature that a pavement exposed in warm climates could reach. As references, SBS rubbery (SBS), acid (B150) and natural gypsum (NG150) bituminous samples have been also included.

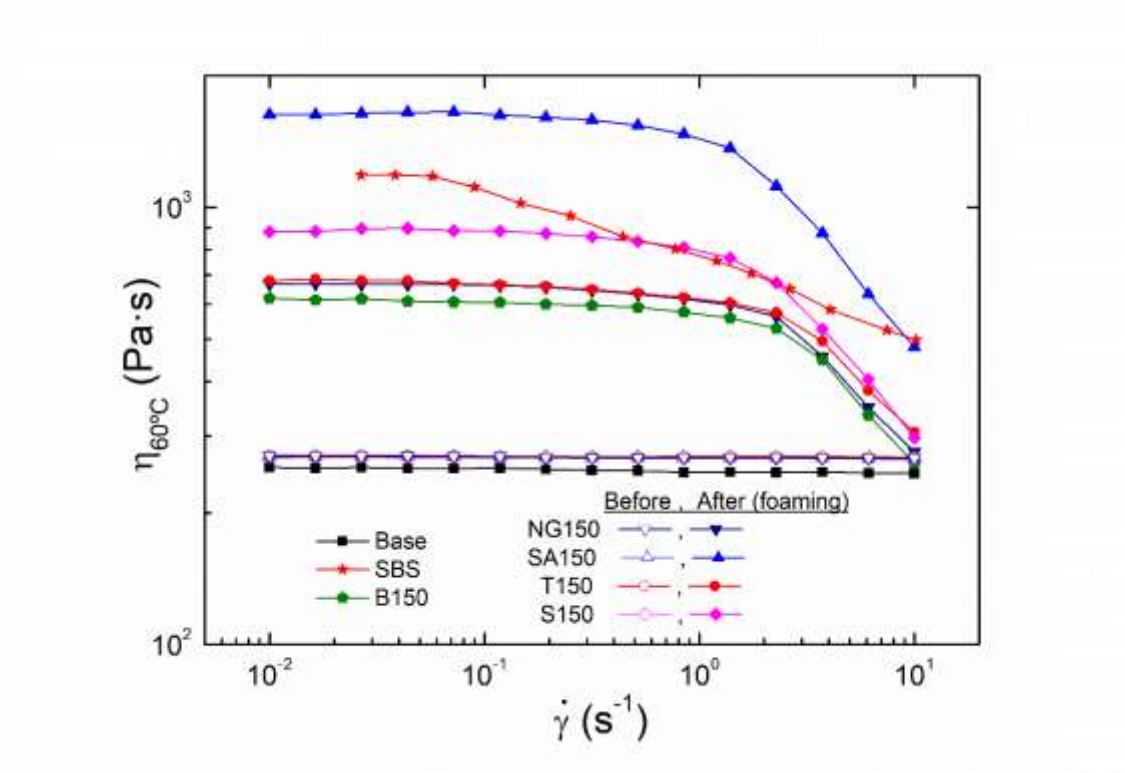

375

376 **Figure 6.** Viscous flow curves, at 60 ºC, for base bitumen (Base), rubbery reference
377 binder (SBS), H_2SO_4/bitumen blend prepared at 150 ºC (B150) and phosphogypsum
378 binders before/after foaming prepared at 150 ºC.

379 It can be observed that base bitumen and bituminous samples before foaming process
380 present a Newtonian response characterized by constant values of viscosity in the entire
381 range of shear rate considered. Thus, the mere addition of FY or NG only produces a poor
382 increase in viscosity, which goes from approximately 250 Pa·s, for the base bitumen, up
383 to 275 Pa·s, for all these modified binders. Interestingly, if a 0.5 wt.% sulfuric acid is
384 added to them, their corresponding residues display a different rheological response. This
385 behaviour is characterized by a Newtonian region at low shear rate with value of viscosity
386 (η_0), followed by a shear-thinning drop when a threshold value of shear rate is surpassed.
387 Interestingly, this change in the rheological response from Newtonian to shear-thinning
388 behaviour reveals the development of a more complex microstructure which is more
389 susceptible to shear rate (Cuadri et al., 2020). Interestingly, although all phosphogypsum-

390 binders before foaming process present the same viscosity at ca. 275 Pa·s, the bitumen
391 modification level achieved by their corresponding residues (referred to as "after
392 foaming" in Figure 6) depends on the phosphogypsum used. This viscosity increase
393 becomes more than one order of magnitude for the residue resulting from the
394 phosphogypsum of Saudi Arabia (SA150), reaching a value of 1650 Pa·s, which is clearly
395 higher than that observed for the rubbery SBS sample (SBS).
396 From a point of view of its final paving application, these results indicate that the AFY
397 phosphogypsum, and at the processing conditions here proposed, would lead to
398 bituminous binders with better resistance to permanent deformations at high in-service
399 temperatures (Biro et al., 2009; Morea et al., 2010) than the rubbery reference SBS-
400 binder.
401 Aiming to quantify the bitumen modification achieved at high in-service temperatures,
402 the values of η_0 has been used to define a modification index, M.I.^{60ºC}, as follows:

403 $$\text{M.I.}^{60°C} = \frac{\eta_{o,binder} - \eta_{o,B150}}{\eta_{o,B150}} \quad (5)$$

404 where "$\eta_{0,binder}$" is the η_0 value of each binder residue and "$\eta_{0,B150}$" that value for the
405 bituminous binder prepared with 0.5 wt.% sulfuric acid at 150 ºC. It is noteworthy that
406 processing temperature (150, 140 or 130 ºC) does not alter the η_0 values for the binders
407 prepared only with sulfuric acid (result not shown). Hence, this index quantifies the
408 viscosity increase in the binder residues due to FY (or NG) addition, regardless the
409 viscosity increase produced by the sulfuric acid bitumen modification.

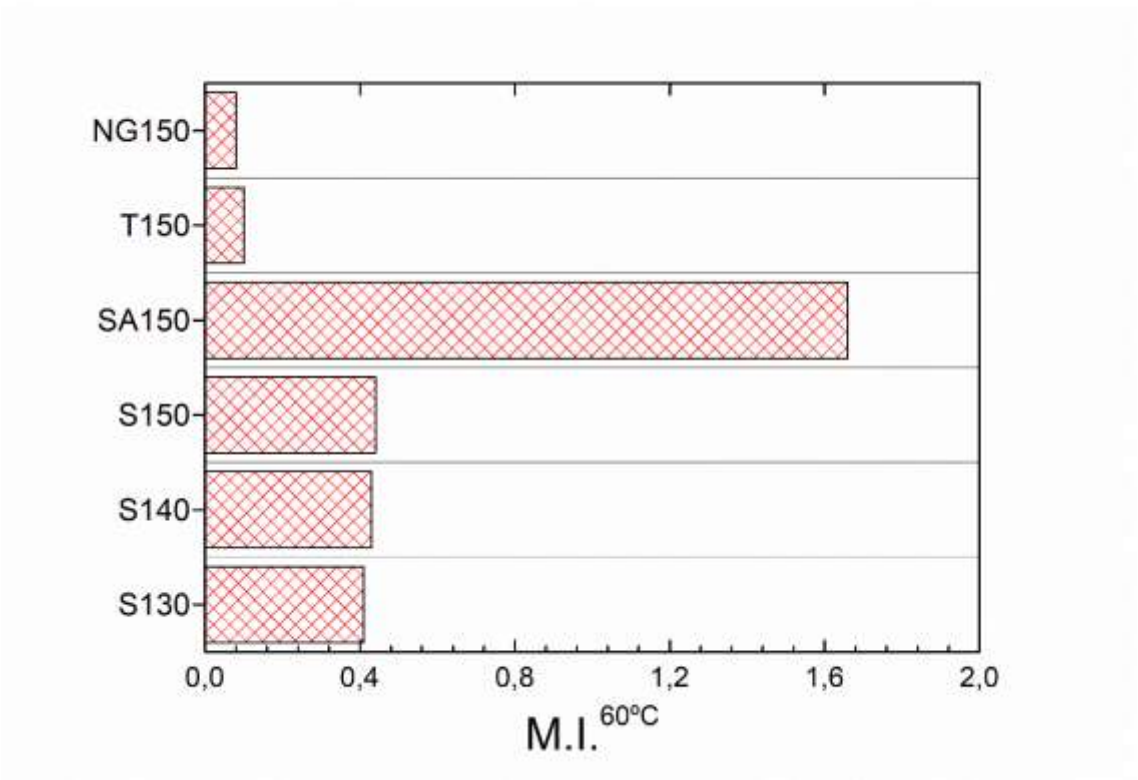

410

411 **Figure 7.** Modification index, M.I.^{60ºC}, for all the binder residues.

412 As deduced from Figure 7, bitumen modification by NG (NG150 sample in Figure 7) or
413 by the FY of Tunisia (T150) only produces a slight viscosity increase in their
414 corresponding binder residues. These values are increased by using the phosphogypsum
415 of Spain at any foaming temperatures (S150, S140 or S130), and the greatest value is
416 observed for binder prepared with the phosphogypsum of Saudi Arabia (SA150).
417 Interestingly, while the foamability of the different phosphogypsum (which was
418 evaluated by the ER_{max} parameter) is related to the structural water content, the viscosity
419 increase noticed on the binder residues can be explained by the amount of phosphorus
420 available for reactions with bitumen's compounds (Giavarini et al., 2000; Masson, 2008).
421 Thus, the AFY phosphogypsum shows the highest phosphorus content (0.74 wt.%),
422 followed by the SFY phosphogypsum (0.22 wt.%), while only traces of phosphorus can
423 be detected in the natural gypsum; however, the TFY phosphogypsum displays its
424 phosphorus associated with apatite mineral and, therefore, there is not free phosphorus

available to react with bitumen's compounds. This fact explains the poor increase in M.I.^{60ºC} values for the AF150 binder residue.

Apart from the viscous flow curves at 60 ºC, temperature sweep tests in oscillatory shear mode were conducted on these samples and plotted in the form of loss tangent (tan δ, which is defined as the ratio of viscous, G'', and elastic, G', moduli), and rutting parameter (|G*|/sin δ) in Figures 8 and 9, respectively. As seen, all samples display, in the temperature interval studied, a predominant viscous character (tan δ > 1), which is more apparent as temperature rises. Interestingly, phosphogypsum binder residues after foaming present enhanced binder elastic properties, since these binders display a decrease in tan δ values compared to base bitumen. Thus, tan δ values for SA150 binder becomes even lower than those observed for the rubbery SBS binder.

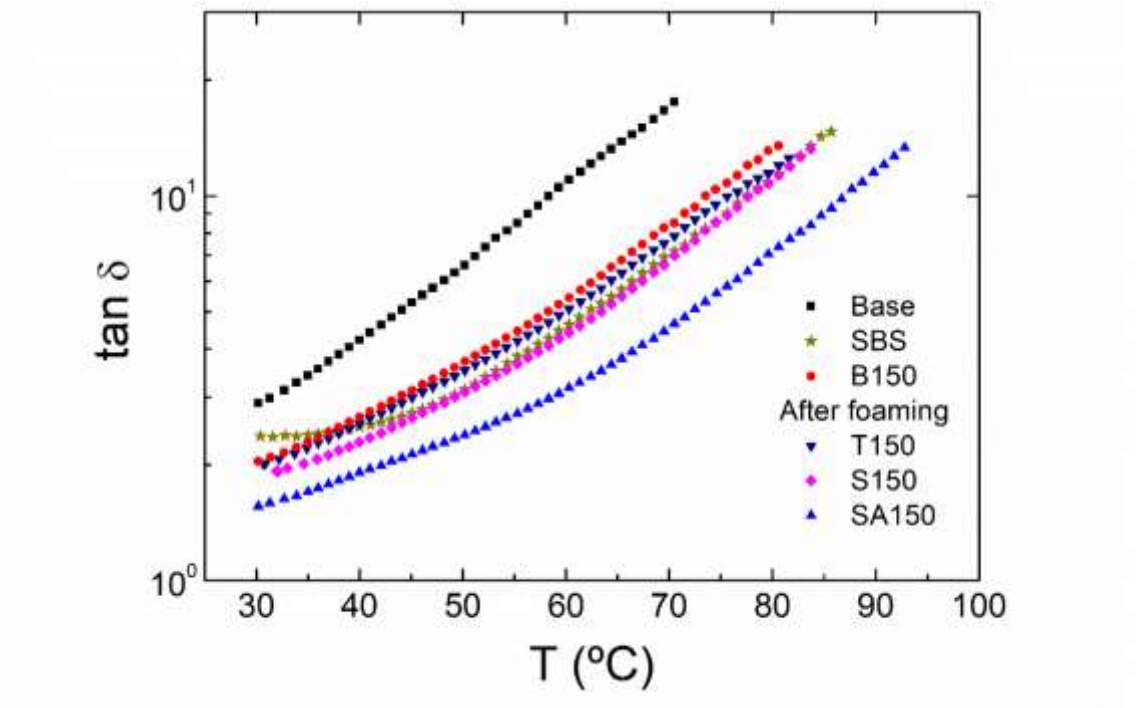

Figure 8. Evolution with temperature of loss tangent (tan δ) for for base bitumen (Base), rubbery reference binder (SBS), H_2SO_4/bitumen blend prepared at 150 ºC (B150) and phosphogypsum binder residues prepared at 150 ºC.

Moreover, the evolution of rutting parameter (|G*|/sin δ) with temperature for these

441 selected binders are displayed in Figure 9. Rutting parameter was considered by Strategic
442 Highway Research Program (SHRP) for evaluating if a bituminous binder meets the
443 rutting resistance requirements at the average seven-day maximum pavement design
444 temperature, being this value the temperature attained when |G*|/sin δ equals 1 kPa.

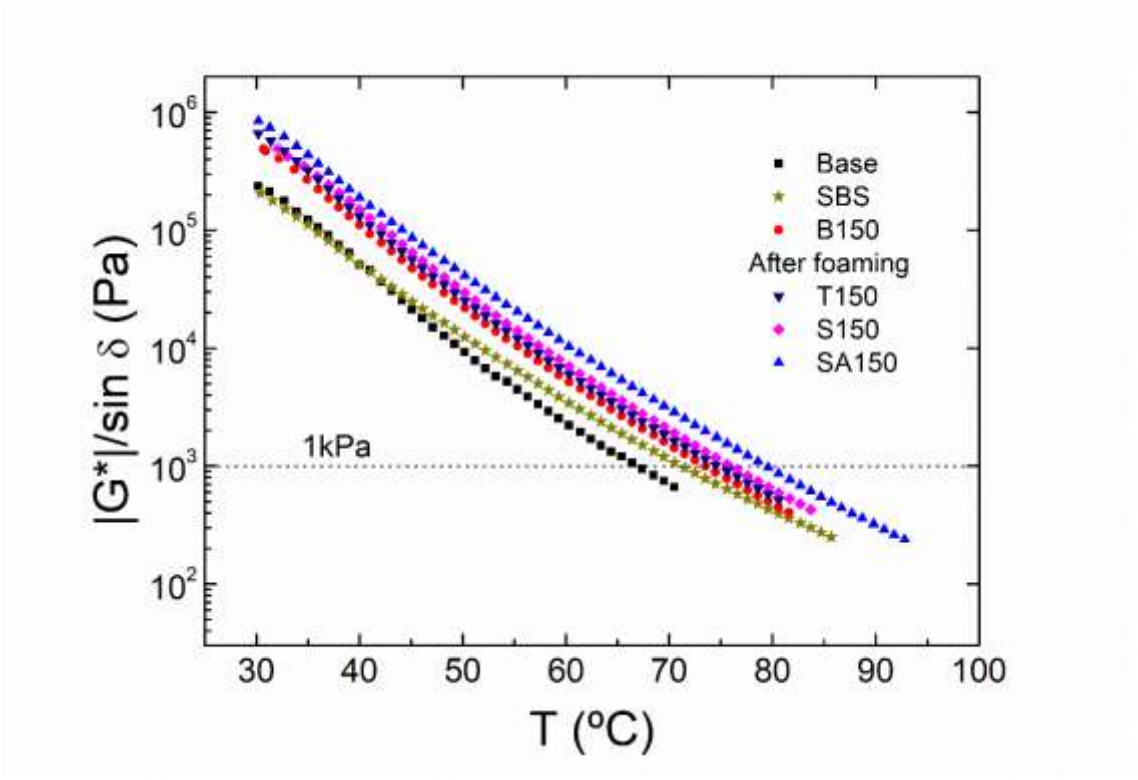

445

446 **Figure 9.** Evolution with temperature of rutting parameter (|G*|/sin δ) for for base
447 bitumen (Base), rubbery reference binder (SBS), H_2SO_4/bitumen blend prepared at 150
448 ºC (B150) and phosphogypsum binder residues prepared at 150 ºC.

449 Thus, calculated temperatures from Figure 9 (which were not obtained from the
450 experimental procedure stated by the standard but it stands for an easy way to establish a
451 comparative analysis) show a significant increase in the resistance to permanent
452 deformation at high in-service temperatures for the phosphogypsum binder residues.
453 Thus, while this limiting temperature (and, therefore, rutting resistance) takes a value of
454 67.2 ºC for the base bitumen, this parameter increases to values of 74.4, 76.5 and 79.1 ºC
455 for T150, S150 and SA150, respectively. These values are even higher than that observed

for the SBS sample (71.9 ºC). These results are in line with those observed from viscous curves at 60 ºC (Figure 6), and again, they make it clear that AFY phosphogypsum would lead to bituminous binders with better resistance to permanent deformations at high in-service temperatures than the rubbery reference SBS-binder.

Finally, phosphogypsum binder residues viscosity at 135 ºC is of particular interest in evaluating the pumpability, mixability and workability of warm mix asphalt (Yuliestyan et al., 2016). Following the standard AASHTO MP320, viscosity at this temperature must be maintained below 3 Pa·s for the binder to be adequately pumped, mixed with the mineral aggregates, and the resulting asphalt mix to be properly laid down and compacted (Silva et al., 2010). Figure 10 shows the viscous flow curves at 135 ºC for these selected binders. In spite of the increases in viscosity at 60 ºC (Figure 6), elastic properties (Figure 8) and rutting parameter (Figure 9) found, the phosphogypsum binder residues fulfil this specification.

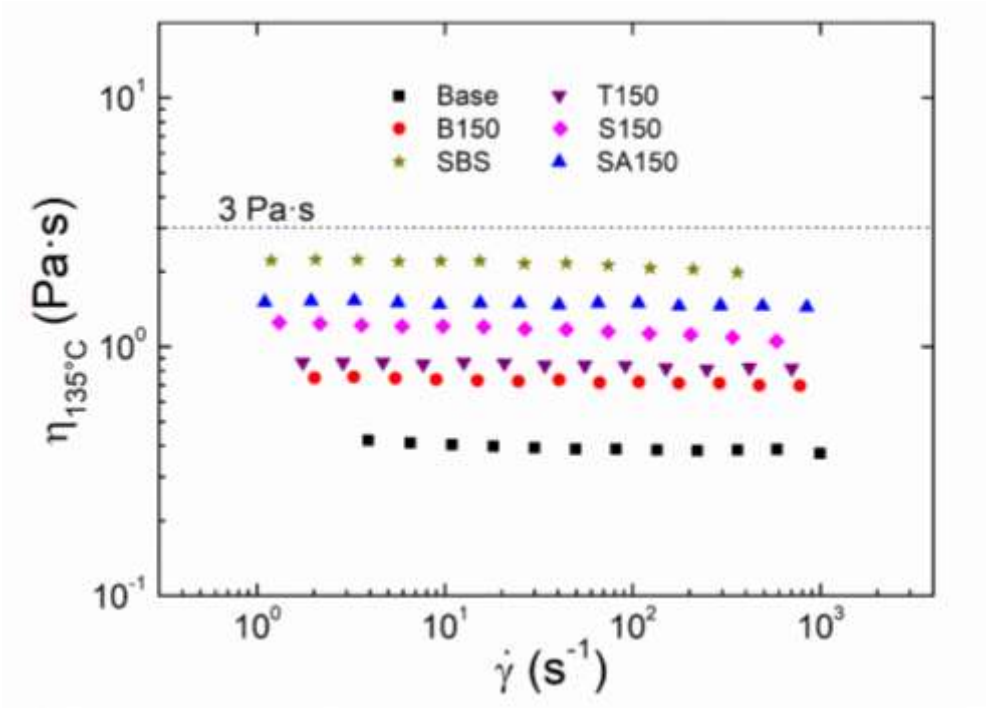

Figure 10. Viscous flow curves, at 135 ºC, for for base bitumen (Base), rubbery reference binder (SBS), H_2SO_4/bitumen blend prepared at 150 ºC (B150) and phosphogypsum binder residues prepared at 150 ºC.

In summary, the foaming process here proposed produces binder residues with enhanced bitumen behaviour at high in-service temperatures (increase in binder viscosity at 60 ºC and enhance elastic properties), and with adequate properties in terms of pumpability, mixability and workability.

3.3. Radiological and environmental implications

Finally, the phosphogypsum binder residues must comply with the radiological and environmental specifications. The European Union (Radiation protection 112, 1999) has proposed to the European countries to control the radioactivity content in building materials when NORM materials are used. The purpose of setting controls on the radioactivity of building materials is to limit the radiation exposure due to materials with enhanced or elevated levels of natural radionuclides. For that, an activity concentration index (I) is defined to ensure that external dose received by population from building do not exceed 1 mSv per year. In this sense, I should be ≤ 1 for materials used in bulk amounts and is defined as follow:

$$I=\frac{C(^{226}Ra)}{300}+\frac{C(^{228}Ra)}{200}+\frac{C(^{40}K)}{3000} \quad (6)$$

where $C(^{226}Ra)$, $C(^{228}Ra)$ and $C(^{40}K)$ are the activity concentrations for ^{226}Ra, ^{228}Ra and ^{40}K, respectively, in the building material considered, expressed in Bq kg^{-1}. The activity concentration of natural radionuclides of FY types, NG and base bitumen are gathered in Table 6.

Table 6. Activity concentration (Bq kg^{-1}) of natural radionuclides of phosphogypsum, types, natural gypsum and base bitumen.

Detection Limit	SFY	TFY*	AFY	NG	BIT	(**)

^{210}Po	0.5	617 ± 13	NM	189 ± 5	13 ± 2	< DL	45
^{234}U	0.5	66 ± 4	129	120 ± 7	11 ± 2	< DL	45
^{238}U	0.5	55 ± 3	113	117 ± 8	12 ± 2	< DL	45
^{230}Th	0.5	466 ± 51	NM	178 ± 6	18 ± 2	< DL	45
^{232}Th	0.5	5 ± 1.6	NM	2.3 ± 0.2	7.2 ± 1.1	1.2 ± 1.0	40
^{210}Pb	13	714 ± 7	316	227 ± 5	16.3 ± 4	< DL	45
^{226}Ra	2.6	536 ± 6	360	213 ± 7	14.7 ± 0.9	< DL	45
^{228}Ra	4.9	6.4 ± 1.6	32	3.7 ± 0.5	8.6 ± 1.3	1.2 ± 1.0	40
^{40}K	20	46 ± 7	80	22 ± 3	327 ± 11	14 ± 5	500

DL: Detection Limit (1 Bq kg^{-1}).
NM: Not Measured.
(*) Uncertainty not given.
(**) Average concentration of natural radionuclides in the Earth crust (UNSCEAR, 2000).

Interestingly, the values obtained for S150, S140, S130, T150, SA150 and NG150 binder residues were 0.17, 0.17, 0.15, 0.13, 0.07 and 0.02 mSv y^{-1}, respectively; consequently, these materials satisfy the criterion established.

On the other hand, the pH and Electrical Conductivity (EC) measured in the eluates of residues obtained at 150 ºC are represented in the Figure 11A and 11B, respectively.

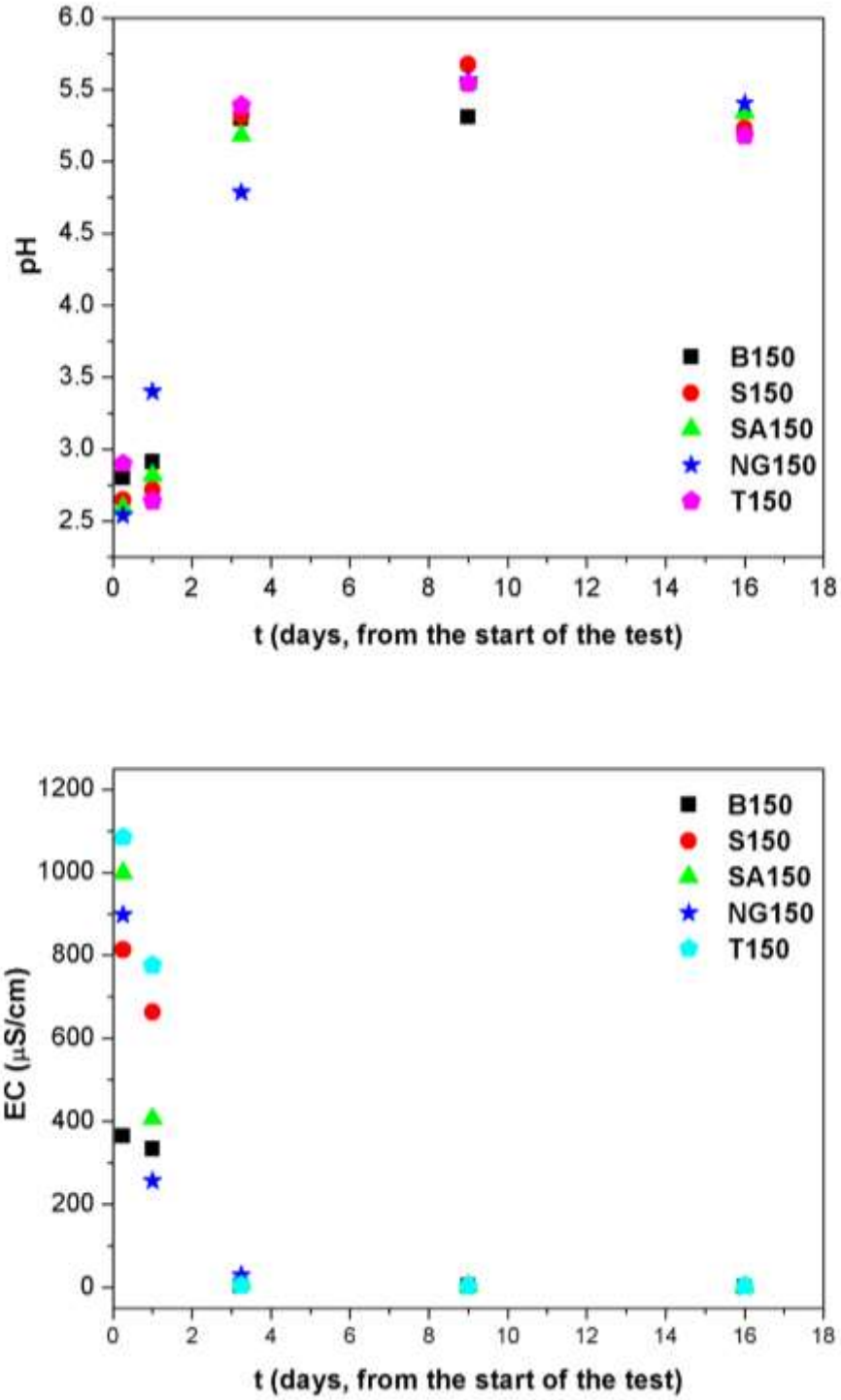

505

506 **Figure 11.** Evolution of (A) pH and (B) EC in eluates of H_2SO_4/bitumen blend prepared
507 at 150 ºC (B150), natural gypsum binder residue (NG150) and phosphogypsum binder
508 residues prepared at 150 ºC.

509 The H_2SO_4/bitumen specimen (B150) pH is about 2.8 and 2.9 in the first and second
510 eluate fraction, respectively, increasing up to 5 in the following lixiviation steps. The

511 natural gypsum binder (NG150) shows a slightly lower value in the first fraction (pH =
512 2.5), progressively increasing in the next steps up to finally a constant value of 5.5. As
513 for the FY residues (S150, SA150 or T150), the first eluates have a pH similar to NG150
514 residue, while in the second eluates the values are closer to ones the found in B150
515 residue, reaching finally a pH = 5.5 that is kept constant in the successive leaching steps.
516 The low pH in the first steps is attributed to the sulfuric acid added to the blends. On the
517 contrary, the EC value decreased with leaching steps, as it is expected. The B150 residue
518 has about 300 $\mu S\ cm^{-1}$ in the two first fractions, reducing drastically to value below 5 μS
519 cm^{-1} in the others. The NG150 sample and FY residues present higher values in the first
520 step, reaching values close to 1000 $\mu S\ cm^{-1}$. In the second eluates, these values are
521 practically halved and continue minimizing to the same values as B150 residue in the last
522 steps. The high EC value in the first fractions indicate a high ions content in solution,
523 reducing as the leaching stages increase.
524 On the other hand, the concentration of the substances in each eluate are shown in Table
525 7, as well as the total released concentration (C_t), the accumulative area released (R_n) and
526 transfer factor (η_j).
527

Table 7. Concentration (ppb) in the eluate in each "i" step, the total released concentration (C_t), the accumulative area released (R_n) and transfer coefficient (η_j) (Uncertainty is given by the standard deviation of two measurements).

Elements	As	B	Ba	Cd	Co	Cr	Cu	Ni	Pb	Sb	Se	Sr	Th	U	V	Zn
B150																
B150–i1	0.73	1.87	0.284	<LD	<LD	0.095	0.938	1.44	0.489	0.039	<LD	<LD	<LD	0.01	0.040	38.1
B150–i2	1.13	2.59	1.765	<LD	<LD	0.388	14.6	1.45	0.760	0.045	<LD	<LD	<LD	<LD	0.032	58.0
B150–i3	0.28	1.57	0.265	<LD	<LD	0.050	0.395	0.099	0.101	0.067	<LD	<LD	<LD	<LD	0.029	21.8
B150–i6	<LD	1.70	0.183	<LD	<LD	0.025	<LD	<LD	0.152	0.025	<LD	<LD	<LD	<LD	0.011	21.1
C_t (ppb)	**2.15**	**7.73**	**2.50**	**-**	**-**	**0.56**	**15.91**	**2.99**	**1.50**	**0.18**	**-**	**-**	**-**	**0.01**	**0.11**	**139**
R_n (mg/m^2)	**0.17**	**0.62**	**0.20**	**-**	**-**	**0.05**	**1.29**	**0.24**	**0.12**	**0.01**	**-**	**-**	**-**	**0.001**	**0.01**	**11**
S150																
S150-i1	2.43	1.97	0.35	<LD	<LD	0.38	4.80	2.93	0.58	0.05	<LD	2.79	<LD	0.01	0.06	41.27
S150-i2	0.87	1.95	2.07	<LD	<LD	0.22	12.96	1.47	0.77	0.04	<LD	<LD	<LD	0.01	0.04	54.23
S150-i3	10.12	1.75	0.75	<LD	<LD	0.02	1.23	0.43	0.24	0.04	<LD	<LD	<LD	<LD	0.02	57.85
S150-i6	2.47	2.17	0.25	<LD	<LD	0.13	0.75	0.13	0.27	0.07	<LD	<LD	<LD	0.01	0.02	30.34
C_t (ppb)	**15.9 ± 4.0**	**7.84 ± 0.63**	**3.41 ± 1.47**	**-**	**-**	**0.75 ± 0.49**	**19.7 ± 5.6**	**4.95 ± 0.74**	**1.86 ± 0.62**	**0.20 ± 0.01**	**-**	**2.79 ± 1.10**	**-**	**0.03 ± 0.01**	**0.14 ± 0.02**	**184 ± 34**
R_n (mg/m^2)	**1.21 ± 0.39**	**0.59 ± 0.09**	**0.26 ± 0.13**	**-**	**-**	**0.06 ± 0.04**	**1.56 ± 1.28**	**0.37 ± 0.03**	**0.14 ± 0.06**	**0.01 ± 0.01**	**-**	**0.21 ± 0.10**	**-**	**0.01 ± 0.01**	**0.01 ± 0.01**	**13.9 ± 3.6**
η_j (%)	**9.42 ± 3.36**	**-**	**0.28 ± 0.17**	**-**	**-**	**0.18 ± 0.16**	**14.4 ± 6.1**	**8.31 ± 1.7**	**1.33 ± 0.63**	**7.43 ± 0.48**	**-**	**0.03 ± 0.02**	**-**	**0.02 ± 0.01**	**0.18 ± 0.04**	**66.3 ± 17.3**
SA150																
SA150-i1	0.89	1.98	1.83	<LD	<LD	0.20	3.43	1.77	0.75	0.06	<LD	3.76	<LD	0.02	0.05	32.22
SA150-i2	0.65	1.85	0.48	<LD	<LD	0.20	0.78	0.54	0.67	0.03	<LD	0.83	<LD	0.02	0.02	56.67
SA150-i3	0.61	2.22	0.25	<LD	<LD	0.29	2.85	0.72	0.50	0.03	<LD	0.59	<LD	0.01	0.02	24.03
SA150-i6	0.13	2.44	0.40	<LD	<LD	<LD	<LD	<LD	0.15	0.01	<LD	0.15	<LD	<LD	0.01	9.45
C_t (ppb)	**2.21 ± 0.05**	**8.49 ± 0.52**	**2.77 ± 1.20**	**-**	**-**	**0.54 ± 0.08**	**7.07 ± 2.78**	**2.67 ± 0.28**	**1.99 ± 0.88**	**0.14 ± 0.03**	**-**	**4.54 ± 2.85**	**-**	**0.05 ± 0.02**	**0.10 ± 0.01**	**122 ± 10**
R_n (mg/m^2)	**0.18 ± 0.01**	**0.68 ± 0.04**	**0.22 ± 0.10**	**-**	**-**	**0.04 ± 0.01**	**0.57 ± 0.22**	**0.21 ± 0.02**	**0.16 ± 0.07**	**0.01 ± 0.01**	**-**	**0.37 ± 0.23**	**-**	**0.01 ± 0.01**	**0.01 ± 0.01**	**9.86 ± 0.83**
η_j (%)	**9.43 ± 2.80**	**-**	**0.52 ± 0.30**	**-**	**-**	**0.54 ± 0.10**	**27.8 ± 5.6**	**18.3 ± 2.4**	**9.58 ± 5.74**	**-**	**-**	**0.19 ± 0.14**	**-**	**0.26 ± 0.09**	**0.05 ± 0.01**	**63.3 ± 7.3**
T150																
T150-i1	0.33	2.62	0.22	<LD	<LD	0.96	2.38	2.99	0.45	0.06	<LD	4.33	<LD	0.01	0.05	10.35
T150-i2	0.82	2.91	0.46	<LD	<LD	0.68	2.52	0.89	0.23	0.05	<LD	0.76	<LD	<LD	0.02	36.76
T150-i3	0.51	2.02	0.89	<LD	0.02	1.46	2.90	0.80	0.31	0.03	<LD	1.26	0.01	0.02	0.04	12.91

T150-i6	5.91	3.89	0.80	0.16	0.65	0.37	2.54	1.28	0.51	0.04	<LD	1.11	<LD	<LD	0.04	31.87
C_t (ppb)	**7.56 ± 5.95**	**11.4 ± 2.0**	**2.36 ± 0.52**	**0.08 ± 0.08**	**0.66 ± 0.57**	**2.75 ± 2.15**	**8.89 ± 0.72**	**5.95 ± 1.86**	**1.11 ± 0.08**	**0.18 ± 0.06**	**-**	**7.46 ± 0.87**	**0.01**	**0.01 ± 0.01**	**0.16 ± 0.01**	**91.9 ± 37.6**
R_n (mg/m^2)	**0.60 ± 0.47**	**0.91 ± 0.16**	**0.19 ± 0.04**	**0.01 ± 0.01**	**0.05 ± 0.05**	**0.22 ± 0.17**	**0.71 ± 0.06**	**0.48 ± 0.15**	**0.09 ± 0.01**	**0.01 ± 0.01**	**-**	**0.60 ± 0.07**	**0.001**	**0.001 ± 0.001**	**0.01 ± 0.01**	**7.33 ± 2.99**
η_j (%)	**6.94 ± 1.72**	**9.13 ± 2.26**	**0.44 ± 0.14**	**0.02 ± 0.01**	**8.93 ± 1.75**	**0.25 ± 0.22**	**9.17 ± 0.90**	**5.79 ± 2.56**	**1.01 ± 0.07**	**-**	**-**	**0.07 ± 0.01**	**0.04 ± 0.01**	**0.02 ± 0.01**	**0.09 ± 0.01**	**1.12 ± 0.65**
NG150																
NG150-i1	2.15	1.85	1.69	<LD	<LD	0.28	13.19	5.14	0.45	0.03	<LD	4.26	<LD	0.01	0.05	22.98
NG150-i2	0.41	1.38	0.27	<LD	<LD	0.05	1.30	1.50	0.23	0.03	<LD	3.01	<LD	<LD	0.01	16.87
NG150-i3	5.37	2.44	0.27	<LD	<LD	0.03	6.60	0.50	0.42	0.11	<LD	2.30	<LD	<LD	0.01	16.41
NG150-i6	0.38	1.74	<LD	<LD	<LD	<LD	<LD	<LD	0.04	0.04	<LD	<LD	<LD	<LD	0.02	4.94
C_t (ppb)	**8.11 ± 2.82**	**7.42 ± 0.28**	**2.24 ± 0.76**	**-**	**-**	**0.34 ± 0.11**	**21.1 ± 9.9**	**7.14 ± 2.48**	**1.00 ± 0.63**	**0.20 ± 0.12**	**-**	**9.56 ± 1.37**	**-**	**0.01 ± 0.01**	**0.10 ± 0.01**	**61.2 ± 7.2**
R_n (mg/m^2)	**0.60 ± 0.18**	**0.56 ± 0.05**	**0.17 ± 0.07**	**-**	**-**	**0.03 ± 0.01**	**1.56 ± 0.66**	**0.53 ± 0.16**	**0.08 ± 0.05**	**0.02 ± 0.01**	**-**	**0.73 ± 0.15**	**-**	**0.01 ± 0.01**	**0.01 ± 0.01**	**4.68 ± 0.82**
η_j (%)	**47.2 ± 12.7**	**-**	**0.15 ± 0.07**	**-**	**-**	**0.10 ± 0.04**	**26.6 ± 17.8**	**5.52 ± 2.71**	**1.59 ± 0.42**	**3.37 ± 1.65**	**-**	**0.08 ± 0.01**	**-**	**0.01 ± 0.01**	**0.03 ± 0.01**	**26.9 ± 4.8**
LD: Detection limit																

The highest concentrations of the substances are found in the three first steps (i1,i2 and i3) in most specimens, corresponding with the high conductivity mention before. Elements such as Cd, Co, Se and Th are below the Detection Limit (DL) in all eluates (DL_{Cd} = 0.1 ppb; DL_{Co} = 0.01 ppb, DL_{Se} = 0.1 ppb and DL_{Th} = 0.01 ppb), while the majority of elements (B, Ba, Cu, Cr, Pb, Sb, U and V) are in similar concentration as in the sulfuric acid residue (B150) (C_B ~ 8 ppb, C_{Ba} ~ 3 ppb, C_{Cu} ~ 16 ppb, C_{Pb} ~ 1.5 ppb, C_{Sb} ~ 0.2 ppb, C_U ~ 0.1 ppb and C_{Zn} ~140 ppb). Furthermore, it stands out the C_t of As in S150, T150 and NG150, being approximately eight and four times higher than the concentration found in B150 sample (C_{As} ~ 2 ppb). Other elements, such as Ni and Sr are also higher that the eluate of the comparison material (C_{Ni} ~ 3 ppb and C_{Sr} < 0.1 ppb). The evolution concentration (µg/L) of the most relevant metals released during DSLT can also be also consulted in Figure 12.

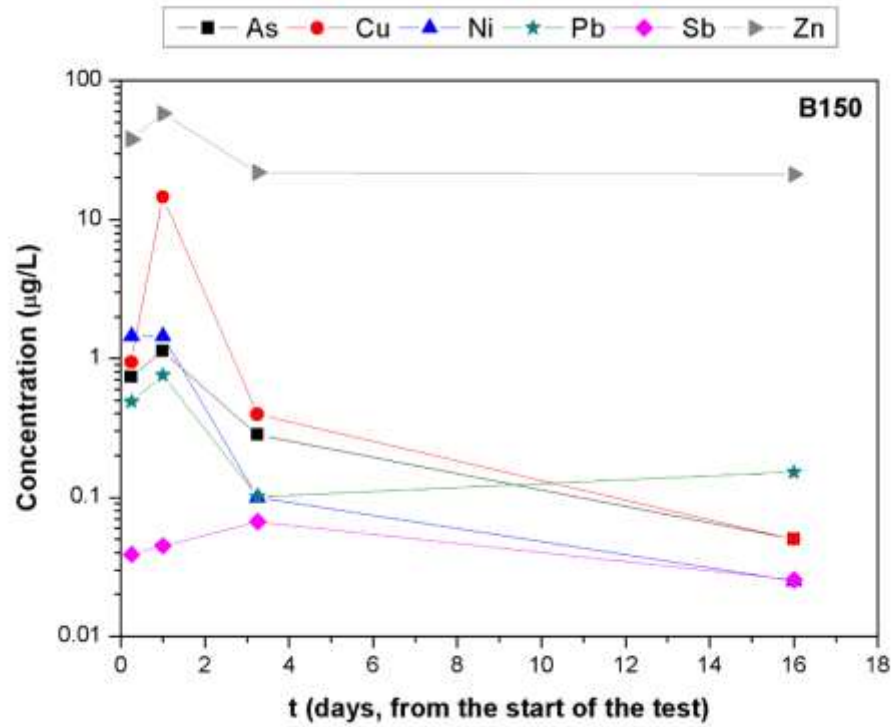
As
Cu
Ni
Pb
Sb
Zn
B150
Concentration (µg/L)
t (days, from the start of the test)

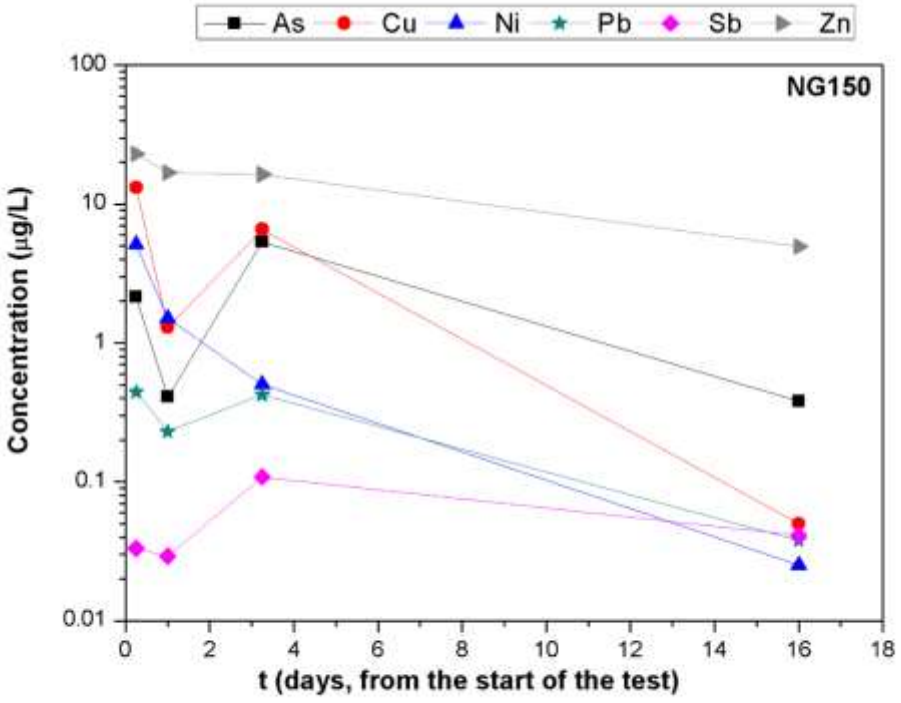
As
Cu
Ni
Pb
Sb
Zn
NG150
Concentration (µg/L)
t (days, from the start of the test)

540

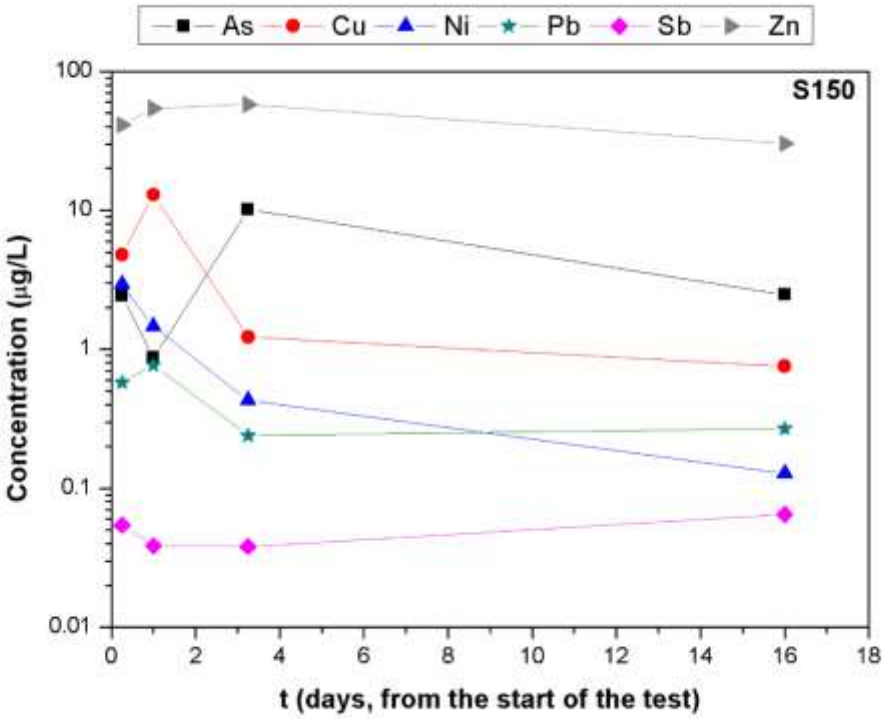
As
Cu
Ni
Pb
Sb
Zn
S150
Concentration (µg/L)
t (days, from the start of the test)

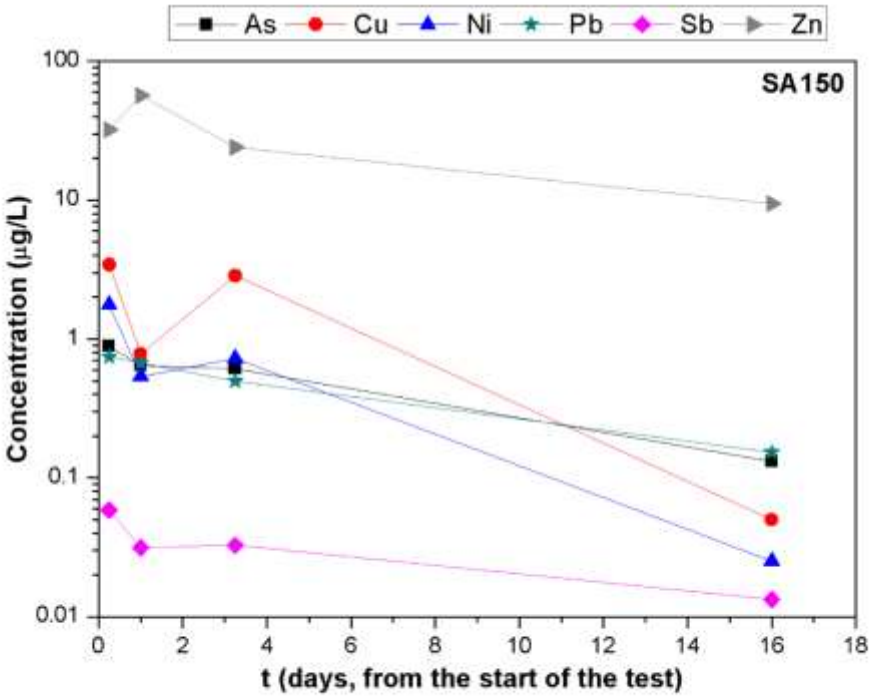
As
Cu
Ni
Pb
Sb
Zn
SA150
Concentration (µg/L)
t (days, from the start of the test)

541

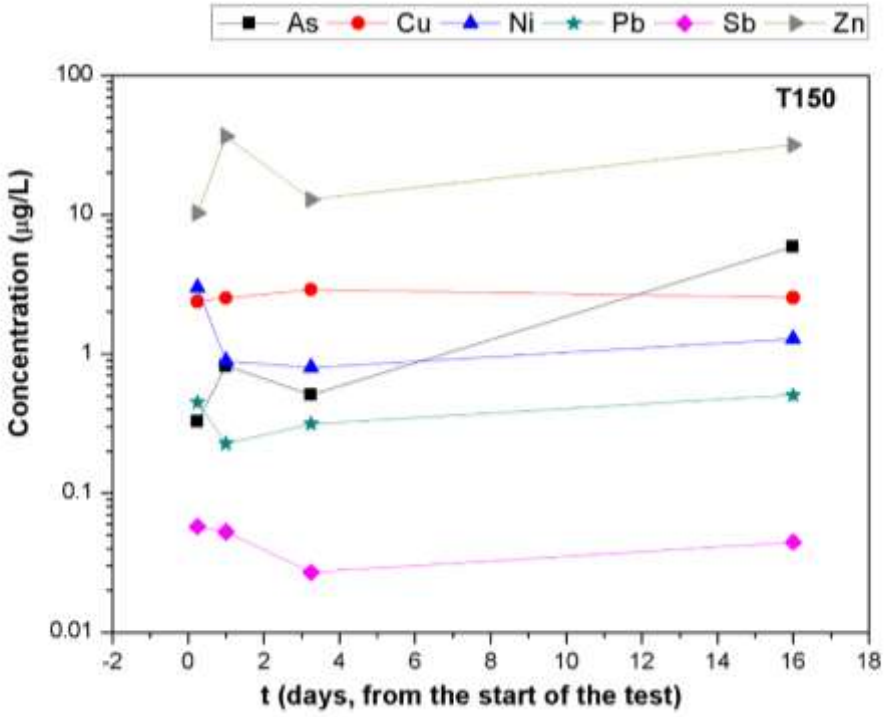

Figure 12. Evolution of concentration (µg/L) of the most relevant metals released during Dynamic Surface Leaching Test (DSLT) for H_2SO_4/bitumen blend prepared at 150 ºC (B150), natural gypsum binder residue (NG150) and phosphogypsum binder residues prepared at 150 ºC.

In general, the R_n of the metals are below 1 mg m^{-2}. Slightly higher values were found for As in S150 (R_{As} ~ 1.2 mg m^{-2}) and Cu, which reaches about 1.5 mg m^2 in S150 and NG150 (R_{Cu} ~ 1.3 mg m^{-2}). Moreover, Zn is the metal that presents the greatest released area, about 14, 11 and 7 mg m^{-2} in S150, B150 and T150, respectively.

The η_j determined for these elements can vary depending on the specimen. The element that shows most significant transferences into the liquid, in descending order, are: NG150: As > Zn > Cu > Ni > Sb > Pb ; S150: Zn > Cu > As > Ni > Sb > Pb ; SA150: Zn > Cu > Ni > Pb > As ; T150: Cu > B > Co > As > Ni > Zn > Pb.

The activity concentrations of natural radionuclides in all eluates fractions of the studied specimens were below the DL (1 mBq L^{-1}).

In view of assessment of the release of the leaching of these materials into the environment, the eluate composition was compared with the regional regulation for Discharges to the Domain Public Hydraulic and Public Maritime-Terrestrial Domain of Andalusia (D 109/2015). According to the limit value of emission, the metals concentration of the eluate of phosphogypsum binder residues here proposed does not exceed in any case the established parameters (As = 1 mg L^{-1}; Cu = 0.75 mg L^{-1}, Ni = 0.6 mg L^{-1}, Pb = 0.22 mg L^{-1} and Zn = 1.5 mg L^{-1}, among others.

4. CONCLUDING REMARKS

The feasibility of use phosphogypsum (FY) waste in the production of foamed bitumen for paving applications was evaluated. To that end, three FYs coming from different fertilizer industries and a natural gypsum were used as foaming agents, including a small quantity of sulfuric acid (0.5 wt.%) in the foamed bitumen formulation. The main conclusions were:

- Results from foaming tests revealed that foaming properties (ER_{max}, t_{max} and foaming rate) clearly depend on two parameters: a) the structural water content of each FY, and b) the foaming temperature. Thus, the optimal foaming temperature was 150 ºC, which would result in a temperature reduction of 20-30 ºC compared to the foamed bitumen by direct addition of water.
- FY foamed binders here proposed present higher stability than those prepared by the standard bitumen foaming (i.e, by water addition to hot bitumen), which allows operators to have more time to conduct the lay-down and compaction operations.
- Viscous flow curves (at 60 ºC) conducted on FY binder residues indicated an improvement in the rheological response compared to the bituminous sample

prepared only with 0.5 wt.% sulfuric acid, whose extent depends on the amount of phosphorus available for reactions with bitumen's compounds.

- FY binder residues satisfy the radioactive specifications when NORM materials are used in building materials, displaying values of activity concentration index (I) much lower than 1 mSv a^{-1}.
- Metals concentration of the eluate for FY binder residues does not exceed in any case the limit value of emission laid down in the regional regulation of Andalusia (D109/2005).

Therefore, the production of phosphogypsum foamed bitumen for asphalt paving applications with enhanced engineering properties and with environmental guarantees, apart from being a sustainable paving practice, may offer an efficient way of immobilizing this radioactive waste.

5. ACKNOWLEDGEMENTS

This research was partially supported by the Spanish Ministry of Science, Innovation and Universities, by projects: (1) ''Fluxes of radionuclides emitted by the PG piles located in Huelva; assessment of the dispersion, radiological risks and remediation proposals" (Ref.:CTM2015-68628-R), and (2) "Equipment for the improvement of the Unity of Environmental Radioactivity of the University of Huelva" (Ref.: EQC2018-004306-P); and Junta de Andalucía, by projects (FEDER 2014-2020): (1) "Procesos básicos que regulan el fraccionamiento y enriquecimiento de radionucleidos n-aturales en condiciones de drenaje ácido de mina" (Ref: UHU-1255876), and (2) "Materiales multifásicos basados en biopolímeros con capacidad de almacenamiento energético para su uso en edificación sostenible" (Ref.: UHU-1256916).

606 **6. REFERENCES**

607 Abreu, L.P.F., Oliveira, J.R.M., Silva, H.M.R.D., Palha, D., Fonseca, P.V., 2017.
608 Suitability of different foamed bitumens for warm mix asphalts with increasing recycling
609 rates. Constr. Build. Mater. 142, 342-353.
610 https://doi.org/10.1016/j.conbuildmat.2017.03.085.

611 Al-Enazy, A.A., Al-Barakah, F., Al-Oud, S., Usman, A., 2018. Effect of phosphogypsum
612 application and bacteria co-inoculation on biochemical properties and nutrient
613 availability to maize plants in a saline soil. Arch. Agron. Soil Sci. 64 (10), 1394−1406.
614 https://doi.org/10.1080/03650340.2018.1437909.

615 Biro, S., Gandhi, T., Amirkhanian, S., 2009. Determination of zero shear viscosity of
616 warm asphalt binders. Constr. Build. Mater.23 (5), 2080-2086.
617 https://doi.org/10.1016/j.conbuildmat.2008.08.015.

618 Bolívar, J.P., Martín, J.E., García-Tenorio, R., Pérez-Moreno, J.P., Mas, J.L., 2009.
619 Behaviour and fluxes of natural radionuclides in the production process of a phosphoric
620 acid plant. Appl. Radiat. Isotopes 67 (2), 345–356.
621 https://doi.org/10.1016/j.apradiso.2008.10.012.

622 Cuadri, A.A., Navarro, F.J., García-Morales, M., Bolívar, J.P., 2014. Valorization of
623 phosphogypsum waste as asphaltic bitumen modifier. J. Hazard. Mater. 279, 11-16.
624 https://doi.org/10.1016/j.jhazmat.2014.06.058.

625 Cuadri, A.A., Navarro, F.J., Partal, P., 2020. Synergistic ethylcellulose/polyphosphoric
626 acid modification of bitumen for paving applications. Mater. Struct. 53, 6.
627 https://doi.org/10.1617/s11527-019-1437-7.

628 de Souza Mendes, P.R., Alicke, A.A., Thompson, R.L., 2014. Parallel-plate geometry
629 correction for transient rheometric experiments. Appl. Rheol. 24, 52721.
630 https://doi.org/10.3933/ApplRheol-24-52721.

631 Dinis-Almeida, M., Afonso, M. L., 2015. Warm mix recycled asphalt – a sustainable
632 solution. J. Cleaner Prod. 107, 310-316. https://doi.org/10.1016/j.jclepro.2015.04.065.
633 Giavarini, C., Mastrofini, D., Scarsella, M., Barré, L., Espinat, D., 2000. Macrostructure
634 and rheological properties of chemically modified residues and bitumens. Energy Fuels
635 14 (2) 495-502. https://doi.org/10.1021/ef9902045.
636 Hailesilassie, B.W., Hugener, M., Partl, M.N., 2015. Influence of foaming water content
637 on foam asphalt mixtures. Constr. Build. Mater. 85, 65-77.
638 https://doi.org/10.1016/j.conbuildmat.2015.03.071.
639 Haque, M.A., Chen, B., Lui, Y.T., Shah, S.F.A., Ahmad, M.R., 2020. Improvement of
640 physico-mechanical and microstructural properties of magnesium phosphate cement
641 composites comprising with phosphogypsum. J. Cleaner Prod. 261, 121268.
642 https://doi.org/10.1016/j.jclepro.2020.121268.
643 He, G., Wong, W., 2006. Decay properties of the foamed bitumens. Constr. Build. Mater.
644 20 (10), 866-877. https://doi.org/10.1016/j.conbuildmat.2005.06.027.
645 Hu, Z., Gao, S., 2008. Upper crustal abundances of trace elements: A revision and update.
646 Chem. Geology 253 (3-4), 205-221. https://doi.org/10.1016/j.chemgeo.2008.05.010.
647 Huang, Y.B., Qian, J.S., Lu, L.C., Zhang, W.S., Wang, S.D., Wang, W.L., Cheng, X.,
648 2020. Phosphogypsum as a component of calcium sulfoaluminate cement: Hazardous
649 elements immobilization, radioactivity and performances. J. Cleaner Prod. 248, 119287.
650 https://doi.org/10.1016/j.jclepro.2019.119287.
651 Kacimi, L., Simon-Masseron, A., Ghomari, A., Derriche, Z., 2006. Reduction of
652 clinkerization temperature by using phosphogypsum. J. Hazard. Mater. 137 (1), 129–137.
653 https://doi.org/10.1016/j.jhazmat.2005.12.053.
654 Karim, A.A., Kumar, M., Mohapatra, S., Singh, S. K., Panda, C.R., 2019. Co-plasma
655 processing of banana peduncle with phosphogypsum waste for production of lesser toxic

potassium−sulfur rich biochar. J. Mater. Cycles Waste Manage. 21 (1), 107−115. https://doi.org/10.1007/s10163-018-0769-7.

Masson, J.F., 2008. Brief review of the chemistry of polyphosphoric acid (PPA) and bitumen. Energy Fuels 22 (4), 2637-2640. https://doi.org/10.1021/ef800120x.

Monat, L., Chaudhury, S., Nir, O., 2020. Enhancing the Sustainability of Phosphogypsum Recycling by Integrating Electrodialysis with Bipolar Membranes. ACS Sustainable Chem. Eng. 8 (6), 2490-2497. https://doi.org/10.1021/acssuschemeng.9b07038.

Morea, F., Agnusdei, J.O., Zerbino, R., 2010. Comparison of methods for measuring zero shear viscosity in asphalts. Mater. Struct. 43 (4), 499-507. https://doi.org/10.1617/s11527-009-9506-y.

Ojovan, M.I., Lee, W.E., 2005. Immobilisation of radioactive wastes in bitumen, in: An Introduction to Nuclear Waste Immobilisation, Elsevier Science Ltd., Amsterdam, pp. 233–244. https://doi.org/10.1016/C2012-0-03562-4.

Perez-López, R., Nieto, J.M., López-Coto, I., Aguado, J.L., Bolívar, J.P., Santisteban M., 2010. Dynamics of contaminants in phosphogypsum of the fertilizer industry of Huelva (SW Spain): From phosphate rock ore to the environment. Appl. Geochem. 25 (5), 705–715. https://doi.org/10.1016/j.apgeochem.2010.02.003.

Pérez-Moreno, S.M., Gázquez, M.J., Pérez-López, R., Vioque, I., Bolívar, J.P., 2018. Assessment of natural radionuclides mobility in a phosphogypsum disposal area. Chemosphere 211, 775-783. https://doi.org/10.1016/j.chemosphere.2018.07.193.

Radiation protection 112, Radiological Protection Principles concerning the Natural Radioactivity of Building Materials. Directorate-General Environment, Nuclear Safety and Civil Protection, 1999.

Rosales, J., Pérez, S.M., Cabrera, M., Gazquez, M.J., Bolívar, J.P., de Brito, J., Agrela, F., 2020. Treated phosphogypsum as an alternative set regulator and mineral addition in

681 cement production. J. Cleaner Prod. 244, 118752.
682 https://doi.org/10.1016/j.jclepro.2019.118752.
683 Silva, H.M.R.D., Oliveira, J.R.M., Peralta, J., Zoorob, S.E., 2010. Optimization of warm
684 mix asphalts using different blends of binders and synthetic paraffin wax contents. Constr.
685 Build. Mater. 24, 1621-1631. https://doi.org/10.1016/j.conbuildmat.2010.02.030.
686 United Nations Scientific Committee on the Effects of Atomic Radiation, UNSCEAR.
687 Sources and Effects of Ionizing Radiation. Report to the General Assembly. 2000.
688 Yuliestyan, A., Cuadri, A.A., García-Morales, M., Partal, P., 2016. Influence of polymer
689 melting point and Melt Flow Index on the performance of ethylene-vinyl-acetate
690 modified bitumen for reduced-temperature application. Mater. Design 96, 180-188.
691 http://dx.doi.org/10.1016/j.matdes.2016.02.003.
692 Zaumanis, M., Haritonovs, V., Brencis, G., Smirnovs, J., 2012. Assessing the potential
693 and possibilities for the use of warm mix asphalt in Latvia. Constr. Sci. 13, 6-59.
694 https://doi.org/10.2478/v10311-012-0008-8.
695 Zrelli, R.E., Rabaoui, L., Daghbouj, N., Abda, H., Castet, S., Josse, C., Beek, P.V.,
696 Souhaut, M., Michel, S., Bejaoui, N., Courjault-Radé, P., 2018. Characterization of
697 phosphate rock and phosphogypsum from Gabes phosphate fertilizer factories (SE
698 Tunisia): high mining potential and implications for environmental protection. Environ.
699 Sci. Pollut. Res. 25 (15), 14690−14702. https://doi.org/10.1007/s11356-018-1648-4.
700